UNIVERSITY OF COPENHAGEN
FACULTY OF SCIENCE

Master Thesis

IDENTIFICATION OF AN UNKNOWN POLYMORPH OF DOCETAXEL AND EVALUATION OF ITS ENCAPSULATION INTO A NANOSTRUCTURED LIPID CARRIER

Academic Advisor:
Heloisa N. Bordallo (Supervisor)
Hery Mitsutake (Co-supervisor)

Written by Nikolaos S. Giannoulis

Submitted: May 20, 2021

Niels Bohr Institute, University of Copenhagen

Acknowledgements

I would like to thank my thesis advisor Prof. Heloisa N. Bordallo, for giving me the opportunity to work on this project and learn so many interesting and useful things for my future carrier, for her patience and support throughout the whole period of this project. I am also grateful for my co-supervisor Dr. Hery Mitsutake for any kind of support during the project. Also, I would like to thank all the staff of the laboratory: from the laboratory technician Marianne L. Jensen who was there to solve and quickly respond to any laboratory issues we had, to the students of the group for the collaborating and supporting environment.

Last, but not least, I would like to thank my family for all the ways they supported me these two years. Whatever I achieve on my journey at the Niels Bohr institute is attributed on them.

Abstract

Breast cancer is one of the most common and fatal types of cancer especially for women, where on average 1 out of 8 will be diagnosed with breast cancer during their lifetime [1]. The universality and the severeness of this illness are the generative power which raised our interest to make this work, that deals with the anticancer chemotherapy drug Docetaxel. Docetaxel is well-known for its chemotherapeutic properties against breast, prostate, non-small lung, and other kinds of local or metastatic cancer [2]. The samples studied in this thesis were kindly provided by Cristália Ind. Farm. Ltda via the post-doctoral student Hery Mitsutake of the University of Campinas (UNICAMP) in Brazil, as part of a collaboration between the two universities.

One of the main issues with Docetaxel is its polymorphism. Due to its different structural appearances, this makes it important, in pharmaceutical perspective, to characterize this drug by means of structural and thermal analysis studies because of the different physicochemical properties arising from such variations in stability and solubility among the different polymorphs [3]. Thus, the aim of this project was to characterize the Cristália Ind. Farm. Ltda non-labeled sample of Docetaxel via a combination of thermal analysis, including Differential Scanning Calorimetry (DSC) and Thermoagravimetric Analysis (TGA) coupled with Fourier Transformed Infrared Spectroscopy (FTIR) complemented by X-Ray Powder Diffraction (XRPD). Moreover, we investigated the properties of Docetaxel intercalated into a nanostructured lipid carrier (NLC). The NLC consisted of Myristil Myristate fatty acid of the ester group, Miglyol (coconut oil) fatty acid of the ester group and the Pluronic (P 188) polymer surfactant. The thermal analysis data was obtained by the Netzch TG 209 F1 Libra Thermogravimetric Analysis (TG) apparatus and the Netzsch 214 Polyma Differential Scanning Calorimetry (DSC) apparatus at the 3rd floor of the H.C.Ø Building (Niels Bohr Institute ward) of the University of Copenhagen. The XRPD data was collected by the Ph.D student Nicolas Pierre Louis Magnard from the Department of Chemistry of the University of Copenhagen. This work is a proof that the combination of different experimental techniques is crucial for full characterization of pharmaceutical raw materials.

Dansk resume

Brystkræft er en af de mest almindelige og dødelige kræftformer, især for kvinder, hvor 1 ud af 8 kvinder i gennemsnit vil blive diagnosticeret med brystkræft i løbet af deres liv [1]. Denne sygdoms universalitet og alvor er den generative kraft, som har vakt vores interesse for at lave dette arbejde, der omhandler kemoterapimedicinen Docetaxel, som er et middel mod kræft. Docetaxel er velkendt for sine kemoterapeutiske egenskaber mod bryst-, prostata- og ikke-små lungekræft samt andre former for lokal eller metastatisk kræft [2]. De prøver, der er undersøgt i denne afhandling, blev venligst stillet til rådighed af Cristália Ind. Farm. Ltda via den postdocstuderende Hery Mitsutake fra universitetet i Campinas (UNICAMP) i Brasilien som led i et samarbejde mellem de to universiteter.

Et af de vigtigste problemer med Docetaxel er dets polymorfi. På grund af dets forskellige strukturelle udseende er det i et farmaceutisk perspektiv vigtigt at karakterisere dette lægemiddel ved hjælp af strukturelle og termiske analyseundersøgelser på grund af de forskellige fysisk-kemiske egenskaber, der skyldes sådanne variationer i stabilitet og opløselighed blandt de forskellige polymorfer[3]. Formålet med dette projekt var således at karakterisere Cristália Ind. Farm. Ltda ikke-emærket prøve af Docetaxel ved hjælp af en kombination af termisk analyse, herunder differential scanning kalorimetri (DSC) og termoagravimetrisk analyse (TGA) kombineret med Fourier Trasformed Infrared Spectroscopy (FTIR) suppleret med X-Ray Powder Diffraction (XRPD). Desuden undersøgte vi egenskaberne af Docetaxel interkaleret i en nanostruktureret lipidbærer (NLC). NLC'en bestod af Myristil Myristate-fedtsyre i estergruppen, Miglyol (kokosolie)-fedtsyre i estergruppen og det polymere overfladeaktive stof Pluronic (P 188). De termiske analysedata blev indhentet ved hjælp af Netzch TG 209 F1 F1 Libra Thermogravimetric Analysis (TG) apparatet og Netzsch 214 Polyma Differential Scanning Calorimetry (DSC) apparatet på 3. sal i H.C.Ø instituttet (Niels Bohr Institut afdeling) på Københavns Universitet. XRPD-dataene for Docetaxel blev indsamlet af ph.d.-studerende Nicolas Pierre Louis Magnard fra Kemisk Institut på Københavns Universitet. Dette arbejde er et bevis på, at kombinationen af forskellige eksperimentelle teknikker er afgørende for en fuldstændig karakterisering af farmaceutiske råmaterialer.

Contents

CHAPTER 1

Introduction

Cancer is one of the most severe and fatal diseases of our time. Breast cancer, particularly, is expected to be diagnosed in more than one out of eight women worldwide during their lifetime [1]. So, it is plausible to consider that "unlocking" of the secrets of such a severe disease is one of the most controversial subjects for many different fields of the scientific community nowadays. This is what raised our interest in studying, in a biophysical perspective, an anticancer chemotherapy material/drug well-known for its effective properties against cancer cells, especially, against breast cancer cells. The subject chemotherapy drug is the so-called Docetaxel (with the commercial brand Taxorate or DTX or DXL). DTX is one of the most commonly used anticancer chemotherapy drugs for treatment of different cancer types, such as: non-small lung cancers, prostate metastatic cancer, etc., but especially for the repression of breast cancer cells [1]. The effectiveness of the drug lies on the fact that it successfully alters the polymerization of the microtubules of the cancer cells, resulting on blocking the mitosis of the infected cells. That results to apoptotic cancer cell death [4]. However, considerable limitations still exist, especially DTX low water solubility (6-7 μg/mL) and its toxicity in healthy cells [5]. To increase solubility, a drug is often formulated in organic solvents, such as dehydrated ethanol and polyoxyethylated castor oil. However, this approach causes many side effects, such as hypersensitivity reactions and hyperlipidaemia [6]. As an alternative, a promising approach is the development of new encapsulation systems for drug delivery. A common methodology is the use of soluble polymeric nano- carriers that allows for controlling the pharmacokinetic and biodistribution of the drug. Under these lines, the biopolymer chitosan has attracted great interest in biomedical applications due to its biocompatibility and biodegradability.[7]

In this project, the DTX carrier is a nanostructured lipid carrier (NLC) made of different lipids (Myristil Myristate and Miglyol coconut oil) and a surfactant (Pluronic 188) provided by collaborators from UNICAMP. We assumed that the intercalation of the drug works protectively for the chemotherapy drug, giving with this, beneficial results for the effectiveness in the "fight" against the cancer cells. The behaviour of the materials was studied using a combination of thermal analysis, including Differential Scanning Calorimetry (DSC) and Thermoagravimetric Analysis (TGA) coupled with Fourier Transformed Infrared Spectroscopy (FTIR) complemented by X-Ray Powder Diffraction (XRPD).

DTX crystallizes in different polymorphs and for this work the determination of which polymorph was used was possible by comparing our XRPD data with online databases using the Mercury- Crystal Structure Visualization, Exploration and Analysis program[8]. TGA data was obtained by heating the samples until 450℃ in order to efficiently capture mass loses and decomposition of the pure materials and the NLC drug carrier. The TGA apparatus is coupled with FTIR spectrometer that allowed us to extend the characterization of the samples by means of the infrared frequency spectrum at which the material absorbs (or emits) the applied heating flow. Subsequently, we used the results of the TG curves to "build" a Kissinger (mathematical) model. This model provides the activation energy or energies, in case of decomposition of multiple agents inside a sample like in our complex sample. Finally, from the DSC data, the appearance of a double peak during an endotherm transition allowed to confirm the presence of two structural phases in our DTX sample.

The impact of our results is discussed in the conclusion of this thesis.

CHAPTER 2

Materials and experimental methods

2.1 Materials

This study focusses on "unfolding" the secrets of an unknown sample of the DTX anticancer chemotherapy drug. A big part of the work includes how the properties of DTX change when this is intercalated into a nanostructured lipid carrier (NLC) that consist of two lipids (one solid and one liquid) and one surfactant, corresponding to the Myristyl Myristate fatty acid, the Miglyol coconut butter and the Pluronic ester P188, respectively. The raw materials used in the preparation of the NLC complex are given in Table 2.1. At this point, immediately, we step into their characterization.

Table 1: Raw materials used in the NLC complex:

Raw material	Supplier
Unknown polymorph	Cristália
Myristil Myristate ($C_{28}H_{56}O_2$)	Croda, BR
Pluronic 188 ($C_8H_{18}O_3$))	Sigma- Aldrich, St. Louis, MO, USA
Miglyol ($C_{39}H_{80}O_{10}$)	Dhaymers Quimica Fina, BR

2.1.1 Docetaxel (Ch. formula: $C_{43}H_{53}NO_{14}$)

Specimens of the Taxus baccata evergreen tree [9] (of the Taxaceae family) (see Fig. 2.1), are used to derive the DTX sample that was used in the experiments of this project.

Figure 2.1: The European Taxus baccata tree with mature and immature cones. Docetaxel is derived for a tree such as this one.[9]

DTX, sold under the brand name Taxotere by Sanofi- Aventi U.S LLC in trihydrate form, is a semisynthetic drug used to treat numerous types of cancer, like, breast, head

and neck, stomach, prostate and non-small-cell lung cancer [1]. It belongs to the taxane family of drugs, which are chemotherapeutic agents that produce antitumor activity by causing stabilization of cellular microtubules, thereby inhibiting cell division [10]. The principal mechanism of action of the taxanes is the disruption of microtubule function. DTX exhibits cytotoxic activity on the target cancer cells by inhibiting their mitosis procedure. So, this drug acts like an inhibitor for the cancer cells' mitotic phase. Until recently, two crystal structures of docetaxel (both considered as trihydrates, but without atomic coordinates) and two derivatives have been reported [3]. A study only few years ago by Vella-Zarb et al. revealed five new crystal forms of DTX (two ethanol hydrated, a monohydrated, an anhydrous and trihydrated form are reported.[3]

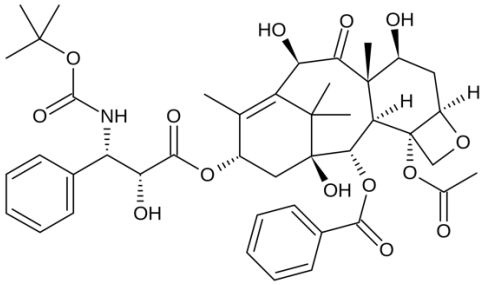

Figure 2.2: Chemical structure depiction of the DTX molecule.[11]

2.1.2 Nanostructured Lipid Carriers (NLCs) [12]

Nanostructured lipid carriers (NLCs) are novel pharmaceutical formulations composed of lipids and surfactants. NLCs hold an eminent potential in pharmaceuticals and cosmetics because of extensive beneficial effects, like skin hydration, occlusion, enhanced bioavailability, and skin targeting. The key attributes of NLCs that make them a promising drug delivery system are ease preparation, biocompatibility, feasibility of scale up, non-toxicity, improved drug loading, and stability. Biodegradable and compatible lipids (solid and liquid) and surfactants are used for the preparation of NLCs. Liquid lipids (oil) incorporation causes structural imperfections of solid lipids leading to a less ordered crystalline arrangement which avert drug leakage and allows for high drug load. These nanocarriers possess the utility in delivery of hydrophilic as well as lipophilic drugs.

Types of NLC [12]

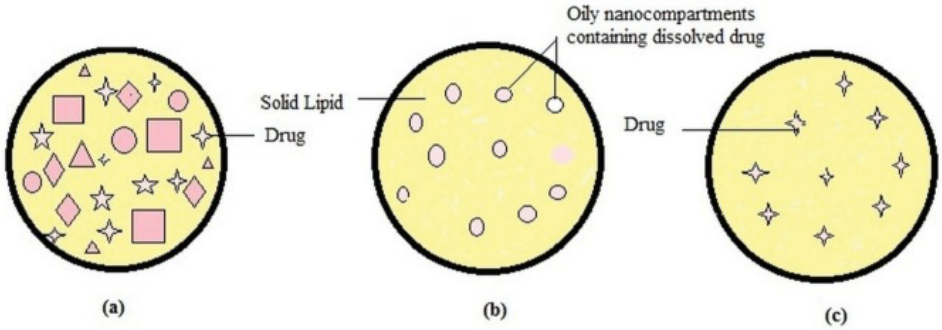

Figure 2.3: Types of nanostructured lipid carrier.[13]

Depending on the location of incorporated drug moieties in NLC, see Figure 2.3 the following three types of morphological models have been proposed:

NLC type I (imperfect crystal model)

Imperfect crystal type NLC consists of a highly disordered matrix with many voids and spaces which can accommodate more drug molecules in amorphous clusters. These imperfections in the crystalline order are acquired by mixing solid lipids with adequate amount of liquid lipids (oils). Due to varying chain length of fatty acids and the mixture of mono-, di-, and triacylglycerols, the matrix of NLC is not able to form a highly ordered structure.

NLC type II (multiple type)- Note that this is the one used in this work

Multiple type NLC is oil/ lipid / water type. Lipophilic drugs, such as DTX, are more soluble in liquid lipids than solid lipids. This idea leads to the development of multiple type NLC using high liquid lipid content. Oil moieties, at low concentrations, are effectively dispersed in the lipid matrix. The addition of oil beyond its solubility induces phase separation forming small nano compartments of oil encircled in the solid matrix. Type II model offer advantages like high drug entrapment efficiency, controlled drug release and minimized drug leakage.

NLC type III (amorphous model)

Amorphous type NLC is formulated by carefully mixing lipids in such a way as to minimize the drug leakage due to process of crystallization. Specific lipids such as hydroxyl octacosanyl, hydroxyl stearate, isopropyl myristate or dibutyl adipate form solid yet non-crystalline particles. The lipid matrix exists in a homogenous amorphous state.

Characterization of NLC [12]

Appropriate techniques are required for characterizing physicochemical properties of NLC in order to ensure their performance, product quality and stability. Various evaluation parameters like particle morphology, interfacial properties, drug entrapment efficiency, crystallinity studies etc. enlighten the workability of NLCs as drug delivery system.

Stability of NLC [12]

One of the most important features of lipid nanoparticles is the ability to decelerate the chemical degradation of actives by photochemical, hydrolytic and oxidative pathways. Chemical stability of drug molecule vastly depends on solid lipid matrix of lipid nanoparticles. Researchers remarked that the chemical stability of NLC fabricated with less crystalline solid lipid and lattice imperfection were improved due to increased drug arrangement within the lipid matrix. Solid state minimizes the exchange of actives with water phase. Moreover, the structure and good chemical stability of lipid itself must be reviewed. Hence, the selection of most suitable lipid during preformulating studies is important. It has been noted in research that actives that are incorporated in the imperfections at the less crystalline lipid matrix of NLC provide prolonged physical stability.

Prolonged effect [12]

Release profile from lipid nanoparticles is drastically influenced by type of lipid (solid or oil) used to formulate the vehicle, concentration of surfactant, solubility and concentration of active in the lipid matrix and method of formulating NLC. NLC are produced by controlled mixing of solid lipids with spatially incompatible liquid lipids leading to special nanostructures with improved drug incorporation and release properties. Targeted drug delivery can be beneficial for potentially reaching the desired state of action and remain there in therapeutic effective concentration for the appropriate time. Poor therapeutic effects & adverse reactions exhibited by conventional topical carriers can be conquered by formulating NLCs.

2.1.3 Composition of the NLC used in this work:

2.1.3.1 Myristyl Myristate (Mirystic acid) (Emp. formula: $C_{28}H_{56}O_2$)

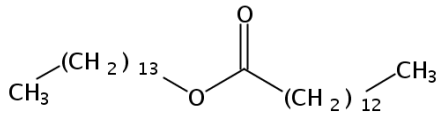

Figure 2.4: Chemical structure depiction of Myristyl Myristate.[14]

It is a solid lipid with a melting point near to body temperature. A schematic of the molecule is given in Figure 2.4.

2.1.3.2 Miglyol (Emp. formula: $C_{39}H_{80}O_{10}$)

Miglyol oil is a saturated liquid lipid derived from coconut oil. Saturated fats lack C=C groups [15]. Fatty (or carboxylic) acids are organic acids that contain a carboxylic group (C(=O) OH) (see Figure 2.5). As a result of tightly controlled manufacturing process microorganisms are practically absent because of very low water levels. They are free of additives such as antioxidants, solvents and catalyst residues. They have a high stability against oxidation.

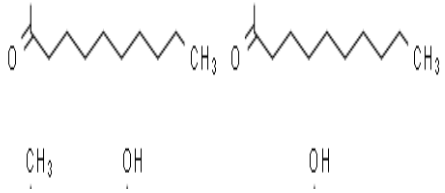

Figure 2.5: Chemical structure depiction of Miglyol.[16]

2.1.3.3 Pluronic 188 (Ch. formula: $C_8H_{18}O_3$)

Pluronics are nonionic triblock copolymers composed of a central hydrophobic chain of polyoxyplopylane framed by two hydrophilic polyoxyethylene chains (see fig.

below). Pluronic (or poloxamer) 188 plays a critical role in protecting cells during cell culture bioprocessing.[17]

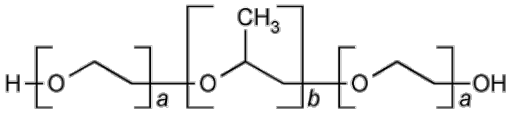

Figure 2.6: Chemical structure depiction of Pluronic 188, where a: oxyethylene (C_2H_4O) and b: oxypropylene (C_3H_6O) copolymer groups with values: a = 80 and b = 27.[18]

NLC preparation method [19]

All materials studied in this work (DTX, Myristil Myristate, Pluronic and Miglyol) were supplied by Dr Hery Mitsutake from the UNICAMP University, Brazil. The samples were in a powder form, appropriate to be used for the devices in the laboratory.

The preparation method of the NLC complex is based, mainly, on four steps:

1. Weight the materials
2. Place in the ultra-turrax
3. Place in the sonicator
4. Cool on ice

NLC without DTX :

1) The first step is to heat water in a 40 mL beaker to a temperature of about 55ºC on the magnetic plate to be used as a water bath. Then, the materials are carefully weighed as follows:

a. In a 20 mL beaker 0.65g of solid lipid (myristyl myristate) are mixed with 0.35g of liquid lipid (miglyol).

b. In another 20 mL beaker, 0.30g of Pluronic 188 is mixed with 10mL of deuterated water.

2) Use the the Ultra-Turrax to obtain a milk-like mixture (as shown in Figure 2.7)

c. The 20 mL beaker containing the Pluronic with the water is placed directly on the hot plate (average of 55°C), under constant stirring, until all the surfactant is dissolved.

d. Concomitantly, the beaker containing the lipids is placed in the water bath at 55°C, under stirring, until the lipids are also completely dissolved. It is important that this beaker always remains in a water bath (at 55°C) until the end of the experiment, as it may precipitate if it cools down.

e. After everything has dissolved (both the P188, and the lipids), the beaker containing the lipids is mixed to the one with surfactant dissolved in water. It will look like milk.

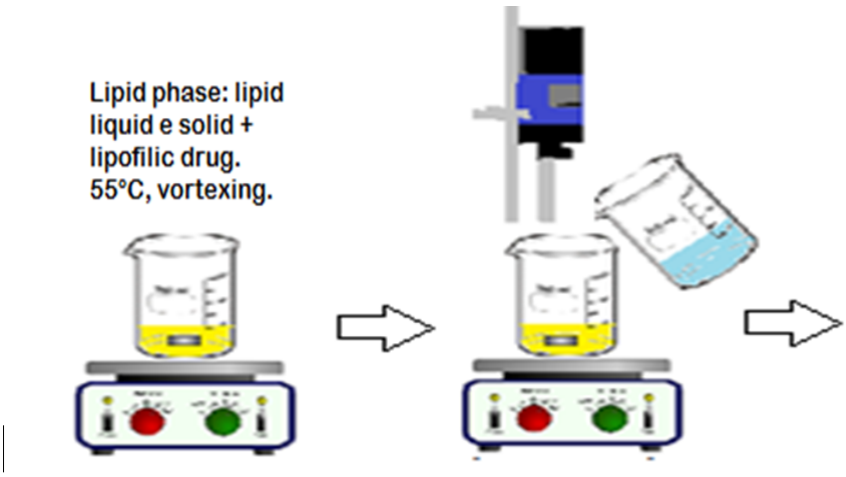

Figure 2.7: Simplified cartoon of the mixture of one beaker containing the surfactant and some specific amount of water (blue) into a beaker containing the lipids (yellow). The necessary stirring machine is clearly highlighted.

3) Sonicator: homogenizing the mixture

f. After the 2 minutes of stirring in the Ultra-Turrax, the sample containing this "little milk" is placed into the sonicator and maintained in a 55°C water bath for 15 min in 30 cycles.

4) Ice: final cooling

g. When the sonication is finished, transfer the "little milk" to a 15ml falcon tube, and dip it into ice to be cooled until it reaches 22°C (on average it takes 6-8 minutes). If it gets too cold, the formulation gets mushy, making it impossible to use.

Incorporation of DTX into the NLC:

To incorporate the drug, weigh the DTX 1% (in relation to water, 0.1 g), together with the solid and liquid lipids. All the rest of the procedure is the same as described above, including the amount of each reagent.

2.2 X- Ray Powder Diffraction [20], [21], [22]

X-Ray Powder Diffraction lies on the field of the X-Ray Diffraction techniques and is one of the most widely applied methods used to characterize crystalline structure of organic materials. When an X-ray is shined on a crystal, it diffracts in a pattern characteristic of the structure. A diffraction pattern plots intensity against the angle of the detector, 2θ, see Figure 2.9 (right). X-ray powder diffraction, where the diffraction pattern is obtained from a powder of the material, rather than an individual crystal, is often easier and more convenient than single crystal diffraction since it does not require individual crystals to be made.

X-rays are partially scattered by atoms when they strike the surface of a crystal. The part of the X-ray that is not scattered passes through to the next layer of atoms, where again part of the X-ray is scattered and part passes through to the next layer. This causes an overall diffraction pattern, similar to how a grating diffracts a beam of light. If beams diffracted by two different layers are in phase, constructive interference occurs and the diffraction pattern shows a reflection, however if they are out of phase, destructive interference occurs appear and there is no reflection. Diffraction reflections only occur if the Bragg's law condition is fulfilled

$$n\lambda = 2d\ sin\theta \quad (1)$$

where,

θ: the diffraction angle of the incident X-Ray

n: the diffraction order (integer: n_1=1, n_2=2, etc.) which counts the spacing of the crystal layers

λ: the wavelength, and

d: the spacing between atom layers

A diffraction pattern can be used to determine and refine the lattice parameters and symmetry of a crystal structure using the Rietveld method [22]. Once the d-spacing of each reflection is obtained by solution of the Bragg equation for the appropriate value of λ, automated search/match routines can be used to compare the d-spacing (or scattering angle) of an unknown material to those of a known material. Files of d-spacings for hundreds of thousands of both organic and inorganic compounds are available from the International Centre for Diffraction Data as the Powder Diffraction File (PDF) [34]. Since crystalline materials have unique diffraction patterns, polymorphs from the same compounds can be identified by using the database of diffraction patterns.

Powder diffractometer

A powder X-ray diffractometer consists of an X-ray source (X-ray tube), a sample holder, a detector and a way to vary angle θ, see Figure 2.8. The X-ray is focused on the sample at some angle θ, while the detector opposite the source reads the intensity of the X-ray it receives at 2θ away from the source path. The incident angle is than increased over time while the detector angle always remains 2θ above the source path.

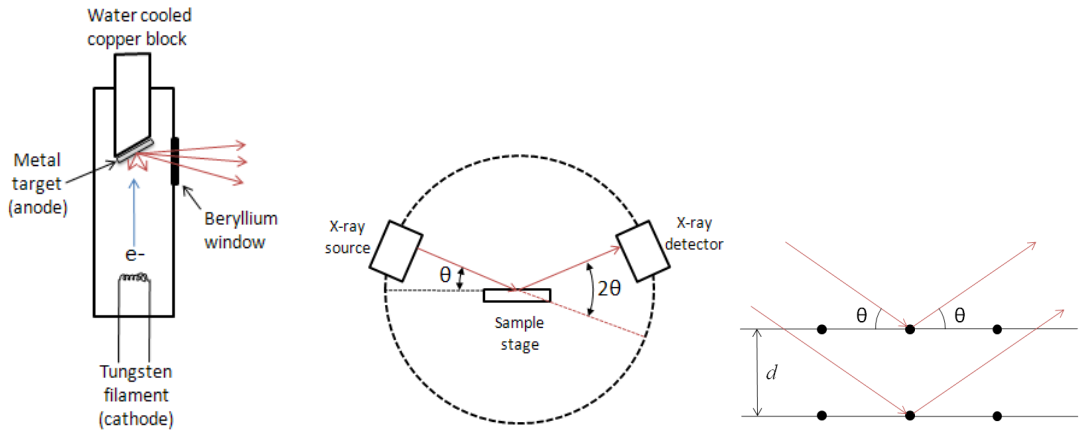

Figure 2.8: Schematic depiction of: (left) the X-Ray tube, (middle) the diffractometer, and (right) the main idea behind the generation of a diffraction pattern and a reflection, particularly, if fulfilling the Bragg law.[22]

The most common source of X-rays is an X-ray tube. The tube is evacuated and contains a copper block with a metal target anode, and a tungsten filament cathode with a high voltage between them. The filament is heated by a separate circuit, and the large potential difference between the cathode and anode fires electrons at the metal target. The accelerated electrons knock core electrons out of the metal, and electrons in the outer orbitals drop down to fill the vacancies, emitting X-rays. The X-rays exit the tube through a beryllium window. Due to massive amounts of heat being produced in this process, the copper block is water cooled.

While older machines used film as a detector, most modern equipment uses transducers that produce an electrical signal when exposed to radiation. These detectors are often used as photon counters, so intensities are determined by the number of counts in a certain amount of time.

The XRPD data of this study was collected by the student Nicolas Pierre Louis Magnard (Department of Chemistry, UCPH). The data was used to identify possible different crystalline phases present of our DTX sample. The XRPD data was collected using a Brucker D8 diffractometer using a Cu Kα source (radiation) in reflection mode, see Figure 2.9 (left). Samples were placed on a zero-background silicon crystal sample holder and XRPD data was collected for 40 minutes on a 2θ range of 5-80°.

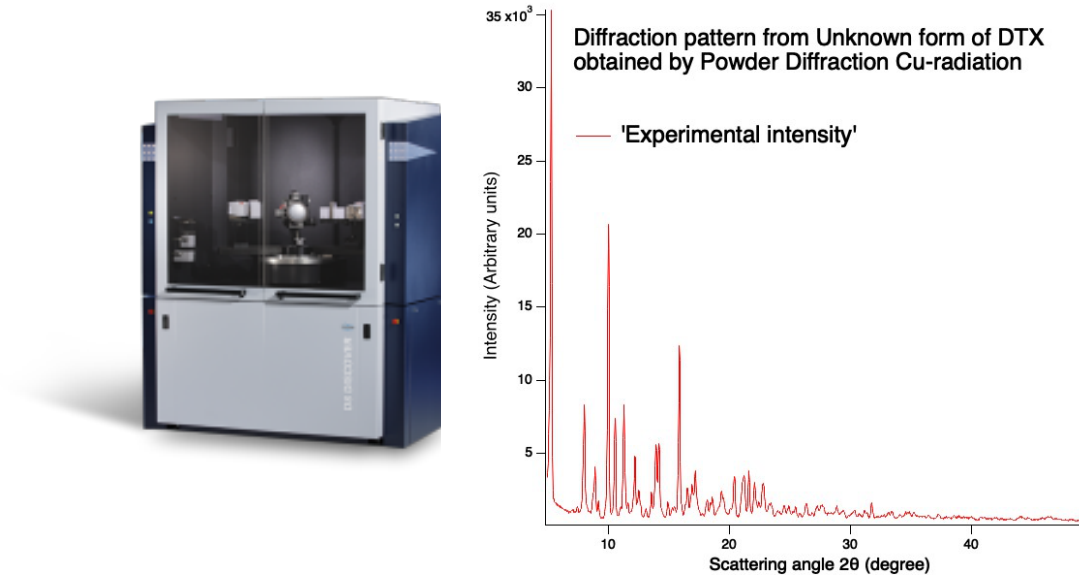

Figure 2.9: (a) Brucker D8 XRD setup.[23] (b) XRD pattern example for DTX. The y-axis represents the intensity and the x-axis the 2θ term shown in equation 1.

2.3 Thermogravimetric Analysis Coupled to Infrared Spectroscopy (TGA- FTIR) [24], [25], [26]

The method for measuring the decomposition or phase transitions of a material is, in principle, simple, and consists of heating the sample to a temperature where it decomposes. Although simple, this technique requires careful measuring conditions throughout the process to generate reliable data and reproducibility.

During a thermal gravimetric analysis (TGA), the sample holder (or alternatively so-called crucible made of Al_2O_3), is placed on a plate connected to a precision balance capable of measuring the change in mass down to hundreds of micrograms. During the experiment, the plate is kept in an electrically heated programmable furnace equipped with a thermocouple to accurately monitor the temperature, see Figure 2.10.

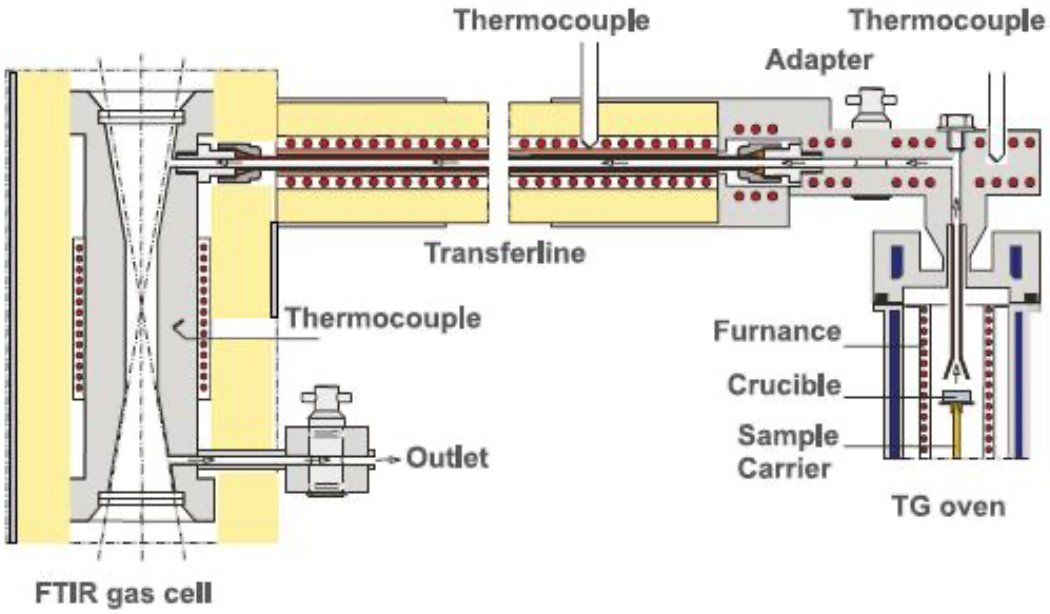

Figure 2.10: Principle of the TGA-FTIR setup. The sample is placed in a furnace on top of a plate connected to a microbalance which measures the change in mass as the sample is heated. Mass loss is dispersed in gaseous form and analyzed by the Fourier Transformed Infrared spectrometer.[27]

The reliability of the TGA holds in the accurate rate of temperature changes as well as in the change in mass during the measurements. Decompositions happen at different energies simply because certain bonds are stronger than others in a molecule. This fact is exploited using this technique by looking at the mass change during heating. When the energy required to activate the weakest bond is reached, the material starts losing mass as parts of the molecule break off, starting slowly as only a few molecules reach the required energy and increasing in speed as more material decomposes. Eventually, it will reach a point where the chemical bonds that hold the molecule together are getting very weak, leading to a drop in the rate at which the mass is lost. Then, the next bonds, if the energy is large enough, start breaking, leading again to the same sort of mass loss. This idea is schematically shown in Figure 2.11.

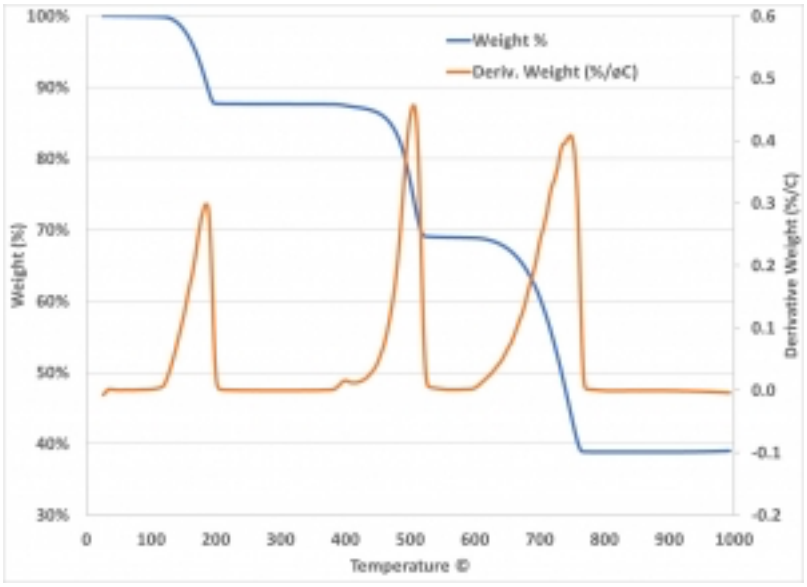

Figure 2.11: A typical TGA measurement for Oxalate, normally used to calibrate a TGA machine, where the weight loss is given in % and derivative weight loss indicates the point where the maximum rate of mass loss happens.[28]

A measurement is first done using the empty crucible to generate a background profile and set the temperature program, which includes the rates at which the sample will be heated and the temperature limit of the measurement. Afterwards, the crucible is placed with the sample inside the instrument and the measurement is done using a defined protocol. While the sample is decomposing, the lost material flows upwards with the air until the gas reaches a FTIR spectrometer where information about the composition of the material can be gained. FTIR is a spectroscopic technique used to identify the functional groups present in organic and inorganic compounds by measuring their absorption of infrared radiation over a range of wavelengths [22], [23]. The FTIR method first collects an interferogram of a sample signal using an interferometer, and then it performs a Fourier transform (a mathematical algorithm) on the interferogram to obtain the infrared spectrum. Finally, it displays the FTIR spectrum of the material.[24] As molecules can vibrate in different ways, for example, by rotating or stretching the interatomic bonds in relation to other atoms in the molecule. These vibrations happen at specific wavelengths depending on what bonds are present, which can be exploited using the FTIR coupled to the TGA system. When the infrared light hits the resonance frequency of the vibrational modes of the molecules, it gets absorbed, and this results in a reduction of intensity of the related frequency in the spectrum. The frequency which would excite a bound state depends on the bond type as well as the mass of the atoms comprising the bond, and thus, the molecule changing the transmission of the infrared signal can be determined. In the following subsection, the procedure for the measurement in this project is detailed.

In this thesis a Netzsch TG 209 F1 Libra thermogravimetric analysis device connected with a Bruker Alpha transmission Fourier-transformed infrared spectrometer was used for the measurements. As mentioned above, the TG device uses small sample holders (crucibles) to load the samples. The crucibles are capable of containing several milligrams of material, depending on the density. After mounting the sample in the

instrument, we define the heating (and cooling) steps of the measurement as well as any additional equipment, such as the FTIR, which is declared to be used for the measurement. In addition, the initial mass of the crucible and the empty crucible are also entered. A typical measurement schedule would include a 5-minute stabilization at the start of the measurement, where the temperature is kept constant (isotherm), followed by an increase in temperature according to the rate used. When the maximum temperature was reached, another 5 minutes of stabilization was done, followed by cooling.

To estimate the activation energy from the observed decompositions, one of the most widely used methods for obtaining kinetic analysis information and, especially, the activation energy, was used the Kissinger model. For that, data were taken at various heating rates of 2.5 $\frac{℃}{\boldsymbol{min}}$, 5.0$\frac{℃}{\boldsymbol{min}}$, 7.5$\frac{℃}{\boldsymbol{min}}$, 10$\frac{℃}{\boldsymbol{min}}$. All samples were weighed with the microgram accuracy weighing device of the laboratory. The weight for all the samples was between 12-16 mg.

2.3.1 Kissinger model [29]

In general, when a material experiences a chemical reaction, it happens at a certain energy called the activation energy. This energy can be used to describe the breakdown of the chemical bonds. Therefore, by finding the activation energy we can quantify to what extent our DTX sample, in its native form as well as intercalated with NLC, are stable. This activation energy can be obtained by the Kissinger model [29] as follows:

The reaction rate for the state transformation can be written as

$$\frac{da}{dt} = A\, e^{-\frac{E}{RT}} f(a)$$

where α is the reacted fraction, A is the Arrhenius frequency factor, T is the temperature in Kelvin (K), R: the gas constant equal to $R = 8.314 \frac{J}{mol \cdot K}$ and $f(a)$ is the kinetic reaction model. For a constant heating rate, denoted β, the previous equation can be written as

$$\frac{da}{dt} = \frac{A}{\beta}\, e^{-\frac{E}{RT}} f(a)$$

During the heating process, the rate of mass loss will increase to a maximum, after which it will decrease due to the reactant being exhausted. The Kissinger method is based on the relation of the activity energy and the temperature at this maximum, and assumes that the second order differential at the point is zero

$$0 = \frac{d^2\alpha}{dt^2} = \left(\frac{E\beta_m}{RT_m^2} + Af'(\alpha_m) e^{-\frac{E}{RT_m}}\right)\left(\frac{da}{dt}\right)_m$$

where the subscript m denotes the parameters at the maximum value, and β_m: the rate $\frac{dT}{dt}$ at which this value was recorded. Rewriting this equation, we obtain

$$\frac{E\beta_m}{RT_m^2} = -Af'(\alpha_m)\, e^{-\frac{E}{RT_m}}$$

The Kissinger model assumes first order reactions, which can be described by the formula $f(a) = (1-a)^n$ with $n = 1$, which then ensures that $f'(\alpha_m) = -1$, leading to the following equation

$$\ln\left(\frac{\beta_m}{T_m^2}\right) = ln\left(\frac{AR}{E}\right) - \frac{E}{RT_m}$$

We can use the above equation in a $\frac{\beta_m}{T_m^2}\ vs\ \frac{1}{T_m}$ plot and obtain the activation energy E in $\frac{kJ}{mol}$ from the slope of the plot which is equal to $-\frac{E}{R}$. Moreover, by taking the intercept we get more information about the pre-exponential factor, which for a first-order reaction is called "frequency factor" and describes how frequently the molecules collide in the system. We can take this from the $\ln\left(\frac{AR}{E}\right)$ in the previous equation.

The Kissinger model requires that the decomposition of the sample follows a first order reaction, which are reactions that proceed at a rate linearly dependent on the concentration of the reactant. If the analysis of our data starts to give unreasonable Kissinger plots, the data must be checked to see if the previous assumption is fulfilled.

2.4 Measurement procedure for Differential Scanning Calorimetry – DSC

Differential Scanning Calorimetry (DSC) is a powerful and commonly used calorimetric method for measuring the thermal properties, such as the enthalpy associated with the process we are investigating, of solid or liquid materials, i.e. phase transitions. DSC is used in many different fields of natural sciences, such as, biophysics, pharmacology, nanoscience, etc [30]. These phase transitions might be for example, see Figure 2.12 (right): melting (T_m-endothermic reaction), crystallization (T_c-exothermic reaction), glass transition (T_g), which is an endothermic process resulting from the presence of amorphous regions in sample, or decomposition/ denaturation (T_g-unfolded state) of the subject material, as the system is losing energy to keep the sample and the reference in the same temperature, as a result of the excess heat the molecules of the material absorb, compare to the empty crucible. The melting transition peak corresponds to a single molecular transition, where ΔC_p is equal to zero.

In other words, DSC results provide information for the sample by measuring the change in heat flow that the material absorbs (or radiates) during the heating procedure, as a function of temperature or time. The corresponding data is collected by measuring cell on top of the furnace, see Figure 2.12 (left). The calorimetric analysis takes place in the inside part of the device. There, there is a furnace which is heated at a constant rate. Then, the heating is transferred in the basis (thermoelectric disk), where two identically made sealed crucibles are placed: one that carries the material, and another one empty (reference sample). These two crucibles are in contact and placed on top of a heating sensor, placed in the basis, that quantifies the heating difference between the crucibles, thanks to the different heat capacity (C_p) of the two samples. All these parts consist of the measuring cell of the device. The heat flow, then, is determined by the thermal equivalent of the Ohm's law:

$$q = \frac{\Delta T}{R}$$

where, q: the heat flow of the sample, ΔT: the temperature difference between the sample and the reference, and R: the resistance of the thermoelectric disk [31],[32]. The enthalpy difference (ΔH) is obtained by integrating the transition area we are interested about. Knowing that C_p is a temperature derivative of the enthalpy

$$C_p = \left(\frac{\Delta H}{\Delta T}\right)_p$$

we can estimate the enthalpy by integrating the C_p, as follows:

$$\Delta H(T) = \int_{T_0}^{T} C_p(T)dT$$

(a)

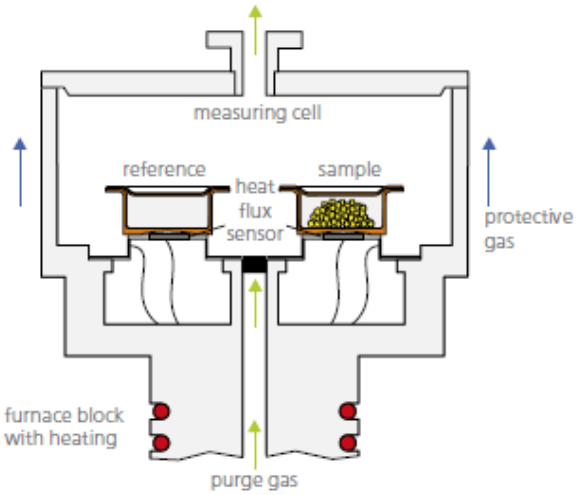

(b)

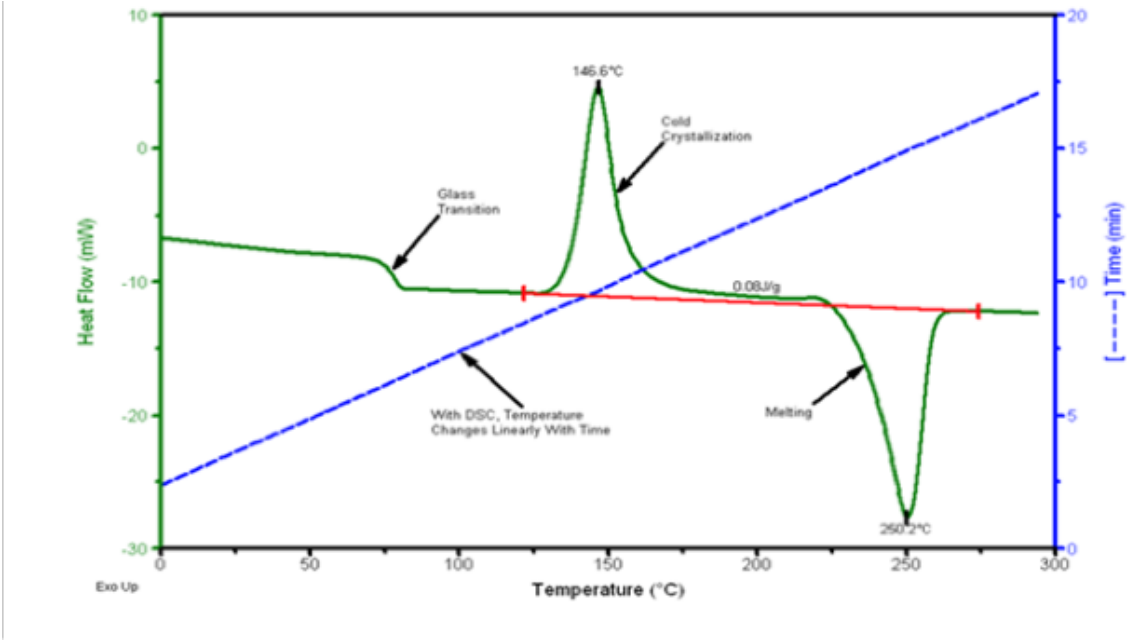

Figure 2.12:(a) Principle of the DSC setup.[33]. (b): A typical DSC measurement: DSC measurement for PET. As we heat the sample, we observe a glass phase transition, followed by crystallization of the material (exothermic reaction) and finally the melting of the material (endothermic reaction) in terms of heat flow (y-axis) over temperature (x-axis) or time (y-axis to the right).[7]

In this work, the DSC analysis was performed using a Netzsch DSC 214 Polyma apparatus. First, we performed temperature calibration by using the melting point and the heat of melting in the following high purity materials: Zinc (Zn), Tin (Sn), and the characteristically high in purity Indium (In). In addition, a heat flow calibration file was used. During the experimental procedure, N_2 gas was purging the atmosphere in the furnace at 40 ml/min. Liquid nitrogen was needed for the cooling.

All samples were weighed with the microgram accuracy weighing device of the laboratory. The weight for all the samples was between 12-16 mg, and transferred into aluminium crucibles, which were, then, sealed. Then, we heated the crucibles within a temperature interval from 28℃ to 192℃ at a constant heating rate of 10 $℃/min$, and then cooling it at a cooling rate of 20 $℃/min$ back to the environmental temperature, again (28℃).

CHAPTER 3

Results and Discussion

Before presenting the results, we recall that the goals of this thesis were to identify the crystal structure of an unknown DTX sample and determine if it was efficiently encapsulated into a NLC formed by two lipids (Myristyl Myristate solid lipid, Miglyol liquid lipid) and a surfactant (Pluronic 188).

The crystalline polymorphs of our Docetaxel sample were characterized by their XRPD diffraction patterns, Differential Scanning Calorimetry (DSC) curves, Thermogravimetric Analysis (TGA) curves, and Fourier-Transformed Infrared Spectroscopy (FTIR).

3.1 X-Ray powder Diffraction results

Crystal structures of DTX trihydrated (DOW3, in red), DTX dehydrated with ethanol solvent (DOW2Et, in black) and DTX hydrated with ethanol solvent (DOWEt, in green) have been obtained by single-crystal diffraction by using synchrotron radiation at low temperature (see Figure 3.1). Furthermore, powder samples of DTX anhydrous (in purple) and DTX monohydrate (in grey) were obtained by powder diffraction using $C_u K_a$ radiation by heating a powder trihydrated DTX (DOW3P) at 383K and 343K, Figure 3.2.

The results of a single crystal X-ray analysis are limited to, as the name implies, one crystal placed in the X-ray beam, while, crystallographic data on a large group of crystals pro vides X-ray powder diffraction information. If the unknown DTX consists of a pure crystalline compound, a simple powder diagram is obtained and by comparing the data with the patterns obtained using the published CIF files we can easily identify the polymorph. To compare the results of full crystallographic analysis, a simple calculation can be done converting the CIF files from the single crystal analysis and powder X-ray diagram to powder diffractograms using Mercury software [8]. This conversion is possible because by means of Rietveld refinement one can determine the unit cell dimensions, space group, and atomic positions. These parameters provide a basis to calculate a perfect powder pattern. Comparing this calculated powder pattern and the powder pattern experimentally obtained, Figure 3.3, will can index the unknown pattern.

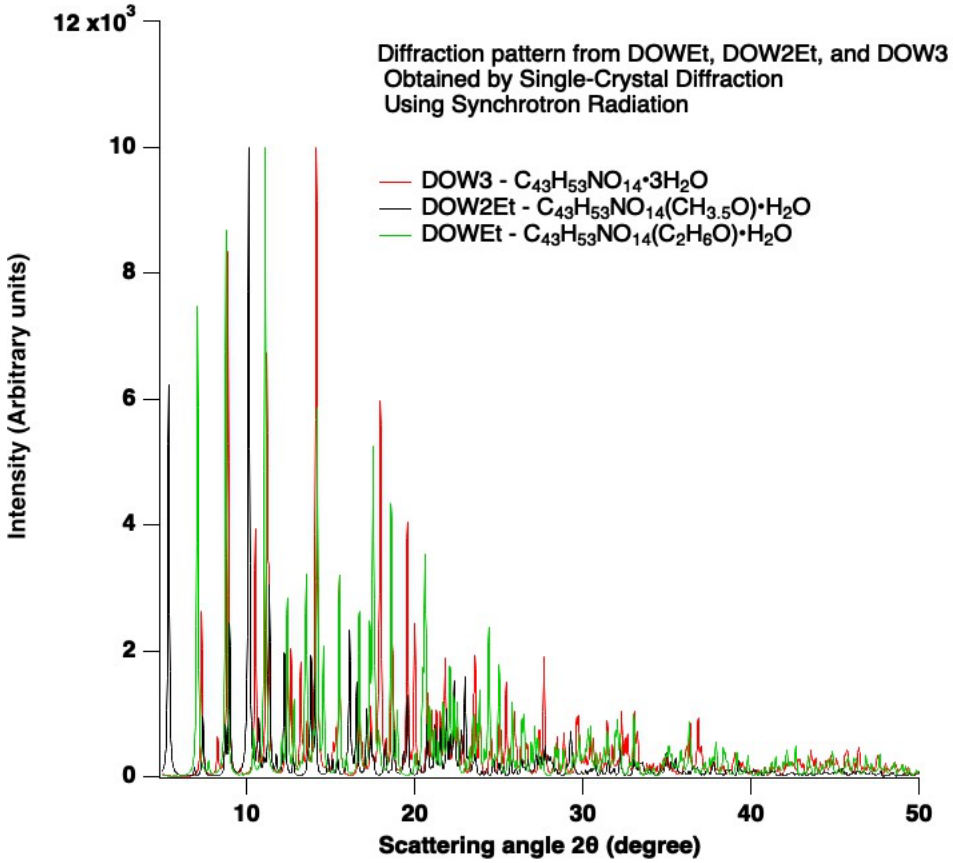

Figure 3.1: X- ray powder diffraction patterns calculated using Mercury software for DTX trihydrated (DOW3, at 150K), DTX dihydrated solvated (DOW2Et, at 120K) and DTX solvated (DOWEt, at 120K), obtained by single-crystal diffraction using synchrotron radiation [3].

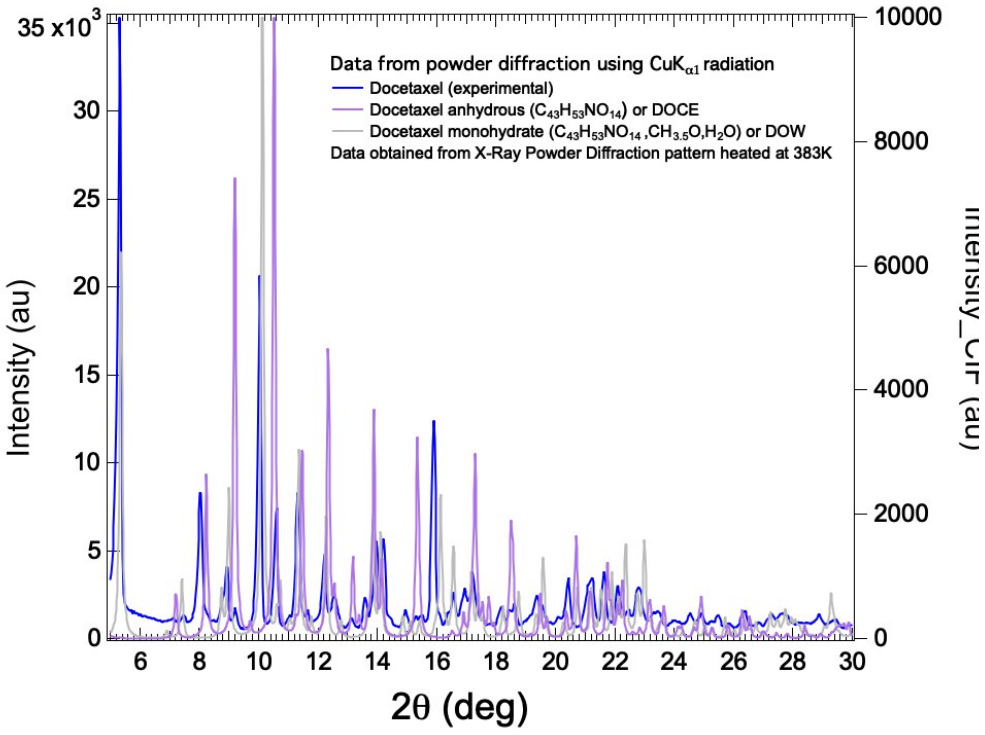

Figure 3.2: X- ray powder diffraction patterns of DTX monohydrated, DTX dihydrated obtained using CIF files [3] using the Mercury software and of the experimetal DTX sample, obtained by laboratory powder diffraction using $C_u K_a$ radiation.

(a)

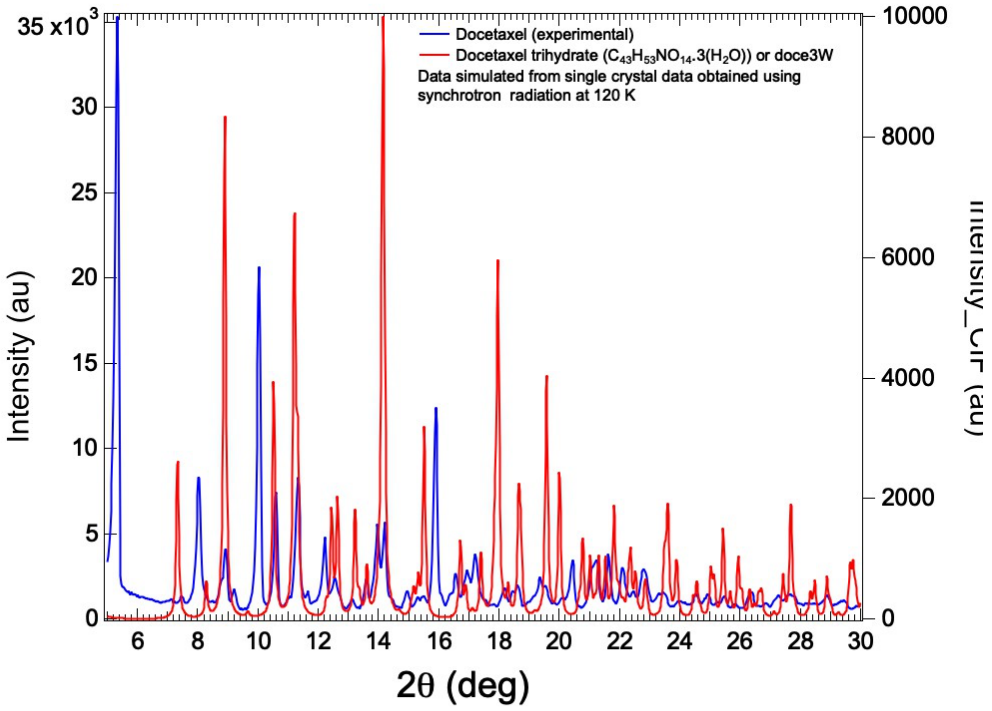
Docetaxel (experimental)
Docetaxel trihydrate ($C_{43}H_{53}NO_{14}.3(H_2O)$) or doce3W
Data simulated from single crystal data obtained using synchrotron radiation at 120 K
35 x10^3
Intensity (au)
Intensity_CIF (au)
2θ (deg)

(b)

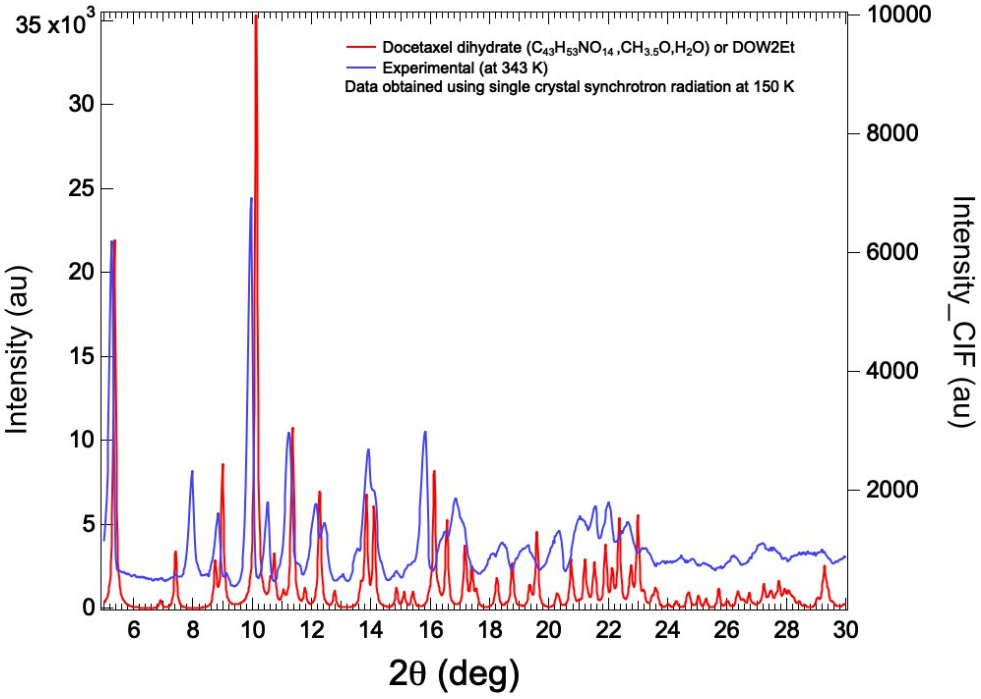
Docetaxel dihydrate ($C_{43}H_{53}NO_{14}$,$CH_{3.5}O$,H_2O) or DOW2Et
Experimental (at 343 K)
Data obtained using single crystal synchrotron radiation at 150 K
35 x10^3
Intensity (au)
Intensity_CIF (au)
2θ (deg)

(c)

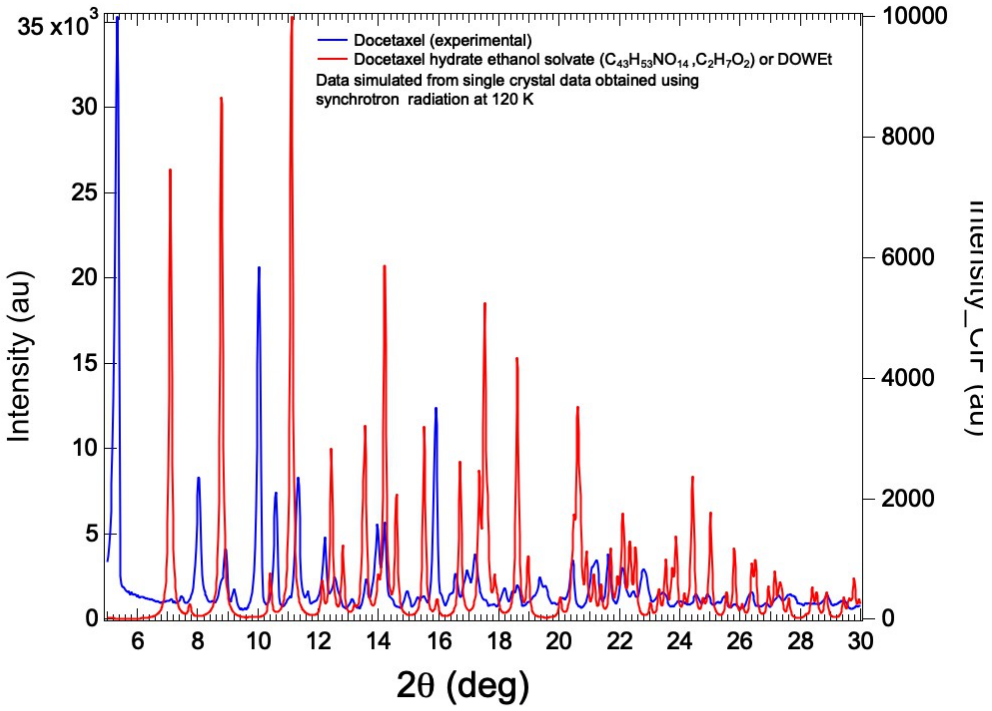
35 x10^3
Docetaxel (experimental)
Docetaxel hydrate ethanol solvate (C43H53NO14,C2H7O2) or DOWEt
Data simulated from single crystal data obtained using
synchrotron radiation at 120 K
Intensity (au)
Intensity_CIF (au)
2θ (deg)

(d)

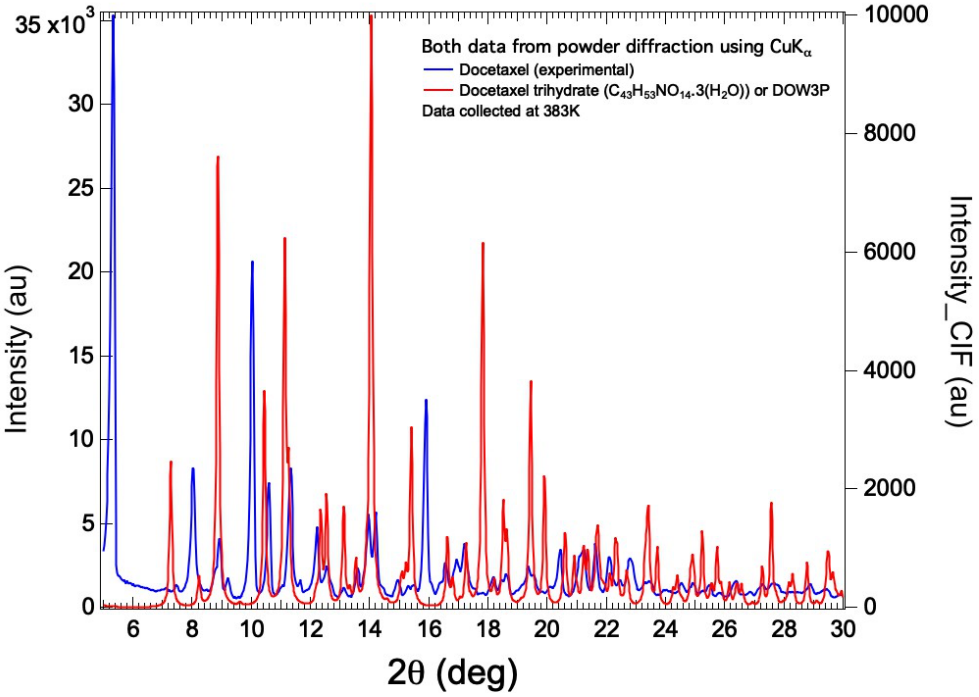
35 x10^3
Both data from powder diffraction using CuKα
Docetaxel (experimental)
Docetaxel trihydrate (C43H53NO14.3(H2O)) or DOW3P
Data collected at 383K
Intensity (au)
Intensity_CIF (au)
2θ (deg)

(e)

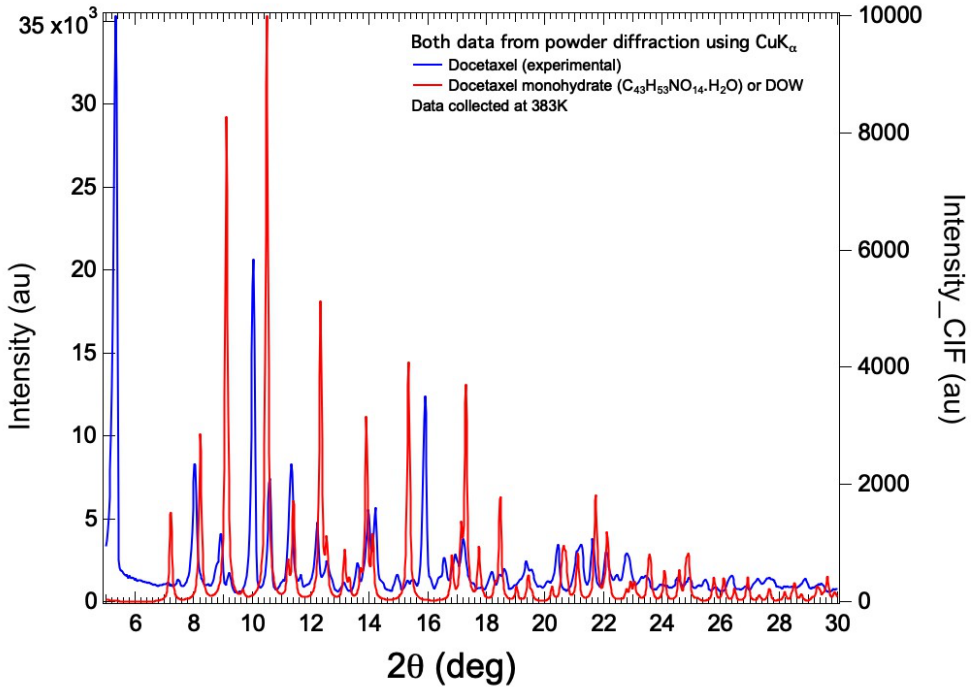

(f)

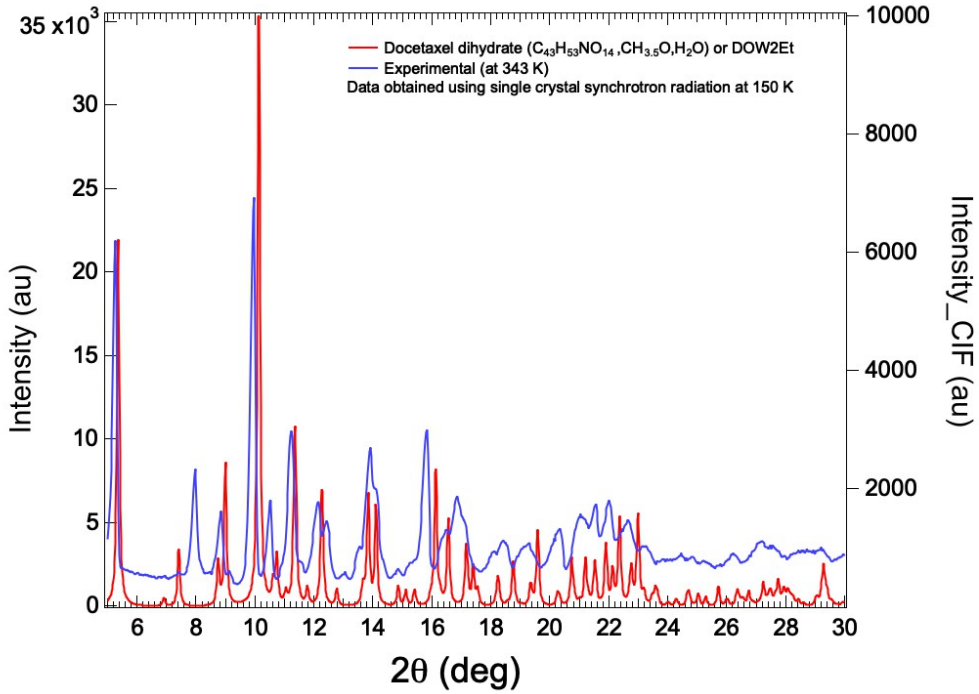

Figure 3.3: Comparison of each known DTX form (red) with the experimental DTX diffraction pattern for DTX (blue). Note that for clarity the figures are represented in two y-axis, on the right we show the intensity (in arbitrary units) of the experimental pattern and on the left we show the intensity (in arbitrary units) for the calculated patterns.

Analysis of the powder X-ray diffraction data collected by having intense reflections at diffraction angles 2θ of about 8.0°, 11.3°, 12.5°, 13.8°, 15.4°, 16.9°, 20.3°, and 23.3° revealed two distinct crystal forms: docetaxel dihydrate with ethanol solvent (DOW2Et, Figure 3.3.b), and an anhydrous form (Figure 3.3.b), the only form to show a reflection at 8.0° degrees.

3.2 Thermal analysis – Fourier Transformed Infrared Spectroscopy (FTIR) : Is DTX intercalated using NLC?

3.2.1 Thermogarvimetric Analysis (TGA) and Differential Scanning Calorimetry (DSC)

3.2.1.1 DTX

The DSC results show no sign of a phase transition in the curve until approximately 140 ℃. On further heating, DTX presents double exothermic phase transitions at 162.7 ℃ and 165.6 ℃, corresponding to the melting transition of an anhydrous and a solvated form originating from the polymorphism of our DTX sample. This confirms the XRPD data we collected, which indicated that the sample was composed by two different phases. The total enthalpy (ΔH) of the double exothermic reaction was determined as $\sim 48.8 \frac{J}{g}$. Previously reported studies on the melting point and enthalpy of DTX have shown an endotherm at 158.2℃ corresponding to its melting point which is in a high agreement with our results. For the enthalpy, previous reports of DTX polymorphs have shown an enthalpy value of $\sim 21.8 \frac{J}{g}$ for anhydrous DTX form and an enthalpy value which ranging from $9 \frac{J}{g}$ to $22.5 \frac{J}{g}$ for other forms of the polymorph [38]. That comes very close to our data if we assume that our enthalpy value is given by the sum of two enthalpies, as we phase two consecutive endotherms, corresponding to two different structural phases on our DTX sample.

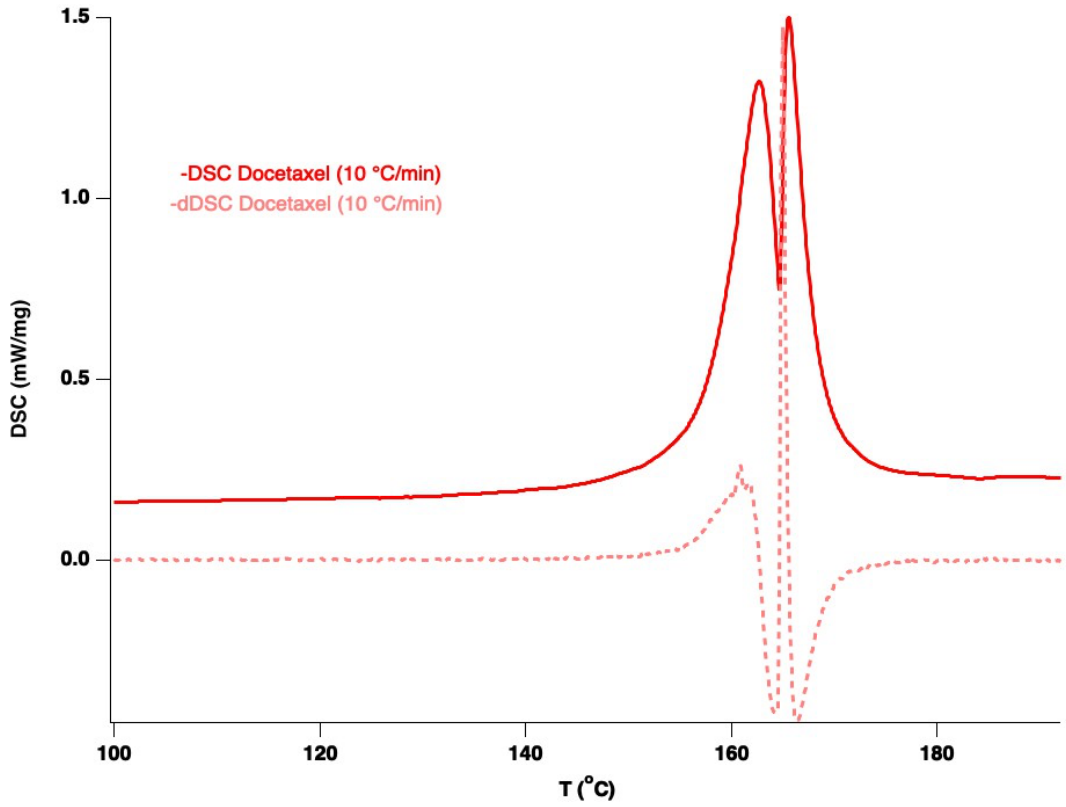

Figure 3.4: DSC and its differential (dDSC) curve obtained by heating DTX from ambient conditions until 192℃. For clarity the data is shown from 100 ℃ to 192 ℃. The experimental results were obtained at a heating rate of 10 $\frac{℃}{min}$. The dDSC interprets the rate of the heating flow giving insight when the maximum and the minimum rates of it, happen.

The TGA and the differential of the TGA (dTGA) diagrams for DTX appear as a gentle mass loss of 1.5% w/w between 60 ℃ and 85 ℃, related, mainly, to evaporation of the ethanol solvent (it is known that the ethanol melting point is at 78.37℃). Sanofi ensures for TAXOTERE 20 mg/0.5 ml a premix concentration of 10 mg/ml docetaxel with 0.097 g/mL, of them, ethanol [35]. So, commercial DTX consists of approximately 1% w/w ethanol, which is very close to our results obtained for the sample provided by Cristália Ind. Farm. Ltd. On further heating, higher levels of mass loss are, majorly, observed above 180 ℃, which are related to decomposition of the DTX. This is in agreement with the literature [35]. The dTGA analysis gives insight when the maximum rate of decomposition occurs, which, for the DTX occur between 188 ℃ (for heating rate of 2.5 $\frac{℃}{min}$) and 209.2 ℃ (for heating rate of 10 $\frac{℃}{min}$).

(a)

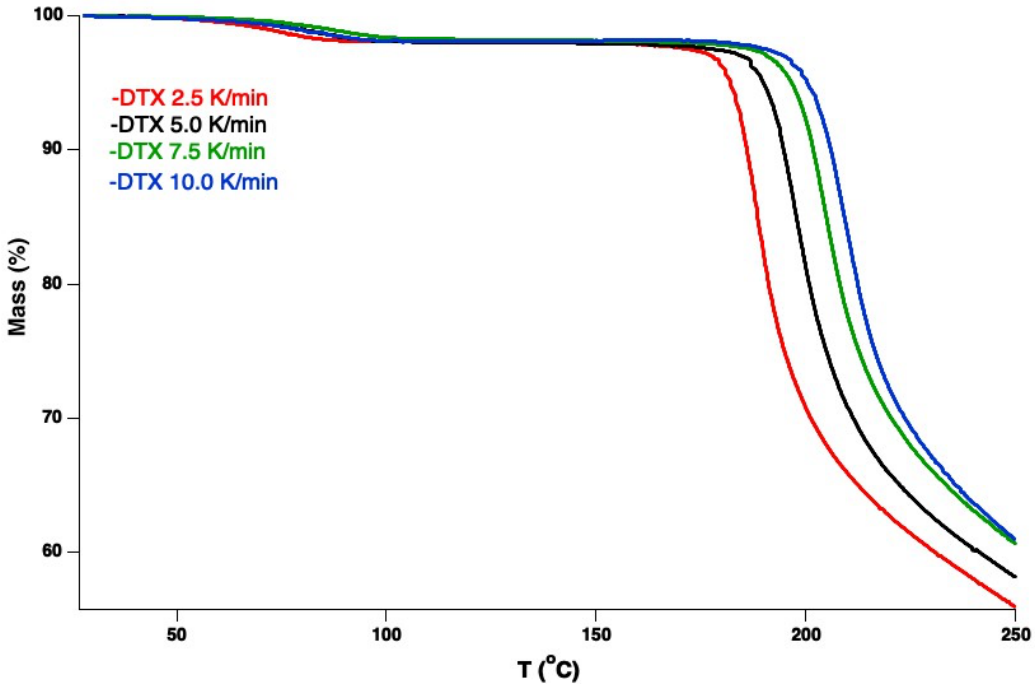

(b)

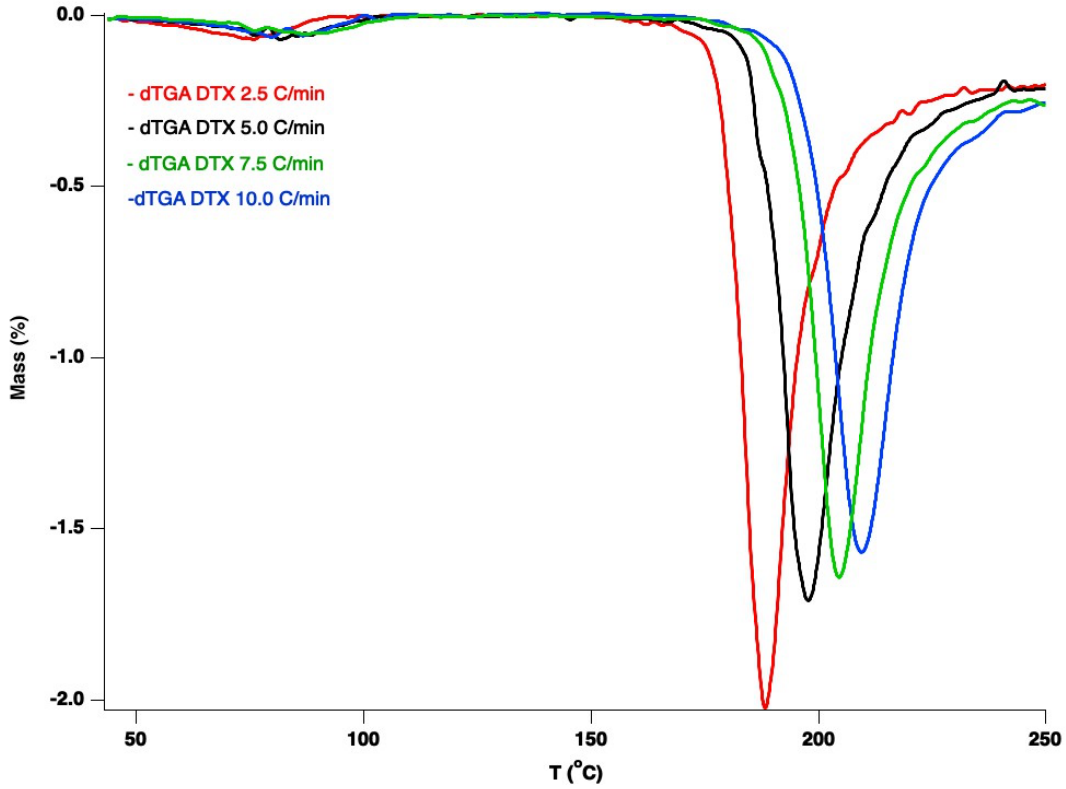

Figure 3.4: (a): Mass loss curves (TGA) of DTX using four different rates from ambient temperature until 250 ℃. Note the ordering of the curves going from the lowest rate losing the most mass per ℃ to the highest rate losing the least mass per ℃. (b): Differential of the mass loss curves (dTGA) for DTX. The differential sets clearer the rate of mass loss per ℃.

The differential of the TGA data for the pure DTX is seen in figure (Figure 3.4.b). The minima shift towards higher values for faster rates happens because the mass loss relative to temperature is expected to be faster for lower rates since they spend longer time at the temperatures where the molecular bonds are activated, and plotting this by using the Kissinger model results in a straight line (see Figure 3.5). The value of the activation energy is 107.4 $\frac{kJ}{mol}$. It is reported that the mean activation energy of degradation of drug- like molecules is 98.6 $\frac{kJ}{mol}$ which is very close to our results [39].

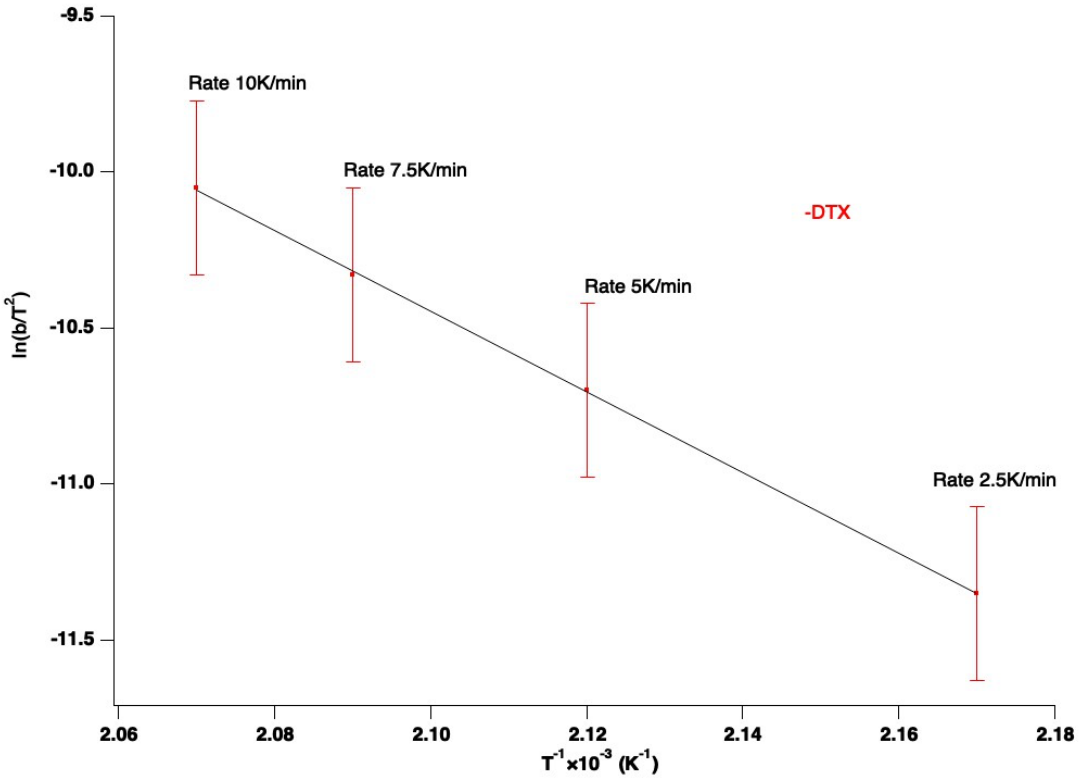

Figure 3.5. The Kissinger plot with a fitted line for the first minima corresponding to the decomposition of DTX, for four different rates (2.5K/min, 5.0K/min, 7.5K/min and 10.0K/min). The straight line shows a fit to the four data points, and the slope of this line is used to calculate the activation energy, as described in Section 2.3.2. The errors were calculated by the formula:

$$\delta\left(x = \ln\frac{\beta}{T_d^2}\right) = \sqrt{\frac{\sum_{i=1}^{i=N}(x_i-\bar{x})^2}{N(N-1)}} = \sqrt{\frac{\sum_{i=1}^{i=4}(x_i-\bar{x})^2}{4(4-1)}}$$

Table 2: Activation energy of the decomposition reaction obtained using the Kissinger model for the DTX. We, also, get data about the starting point of decomposition as well as the percentage of the mass loss after the decomposition reaction.

$\mathbf{T_{rate}}$ $(\frac{℃}{min})$	T_d (°C) (Inset of decomposition)	$T_d^{-1} \times 10^{-3}(K)$	% mass loss	Activation Energy (kJ/mol)
2.5	188.0	2.17	44.17	-
5.0	198.0	2.12	41.95	-
7.5	206.0	2.09	39.55	-
10.0	209.2	2.07	39.38	-
-	-	-	-	107.37

3.2.1.2 NLC and DTX+NLC

The information we obtained from the DTX decomposition data gave many insights about the pure drug, as the decomposition point of the drug and the activation energy of it. Then, we continued making TGA measurements and analysis, with the same approach, on the DTX + NLC complex. However, before that, we needed to get more detail on each compound of the NLC because this information will give us further insight about the different substances decomposed during the heating process. This result is shown in Figure 3.5.

(a)

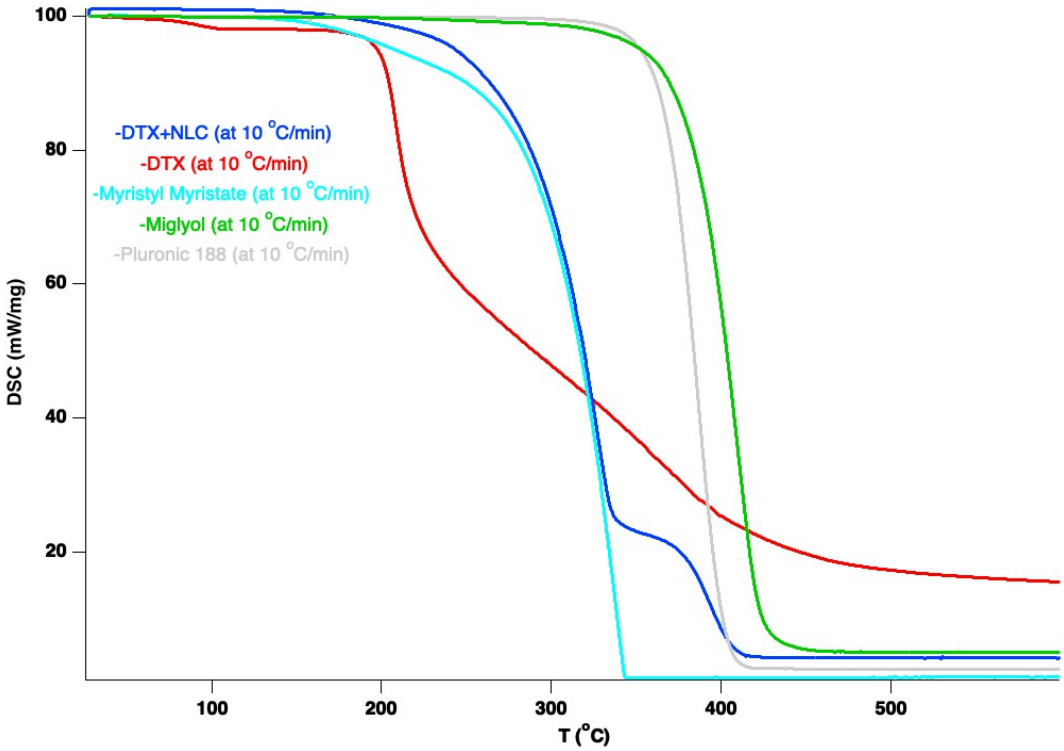

(b)

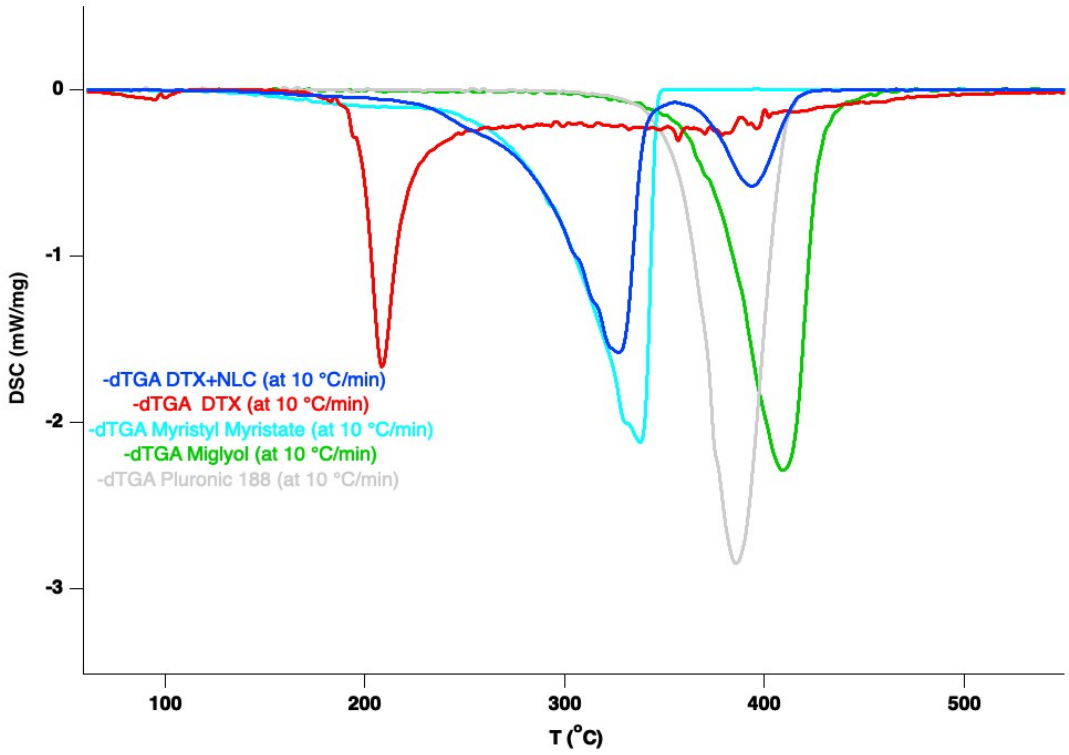

Figure 3.6: TGA (a) and its derivative (dTGA) (b) of DTX (red lines), DTX+NLC complex (dark blue lines), Myristyl Myristate (cyan lines), Miglyol (green lines) and Pluronic 188 (grey lines), using a heating rate of $10\frac{℃}{min}$ from ambient temperature until 600 ℃. In order to highlight the phase transitions the temperature range plotted is from 60 ℃ to 550 ℃ .

From Figure 3.6, we clearly see that the drug is successfully encapsulated into the DTX+NLC complex as the decomposition point of the complex is shifted more than 100℃ compared to the decomposition point of the drug itself. Interestingly, the curves are showing that the decomposition of the complex is almost identical to that of the Myristyl Myristate solid lipid, which is the first compound to decompose from the complex. Moreover, we observe the high stability of the Miglyol liquid lipid and the Pluronic 188 surfactant. The complex appears a second decomposition point around 400℃, a little further than the point where Pluronic 188 is decomposed when measured alone.

From the DSC and dDSC curves for DTX (red lines), DTX+NLC complex (blue), NLC(black), Myristyl Myristate (cyan), Miglyol (green) and Pluronic 188 (grey), Figure 3.7, we observe the phase transitions of the compounds within a temperature interval from ambient temperature to 192°C. Differently from the pure compounds, see Table 3, no further transitions are observed between 56°C-192°C in the complex. The loss of these sharp peaks is a clear sign of amorphization or complexation of the pure drug molecules.

(a)

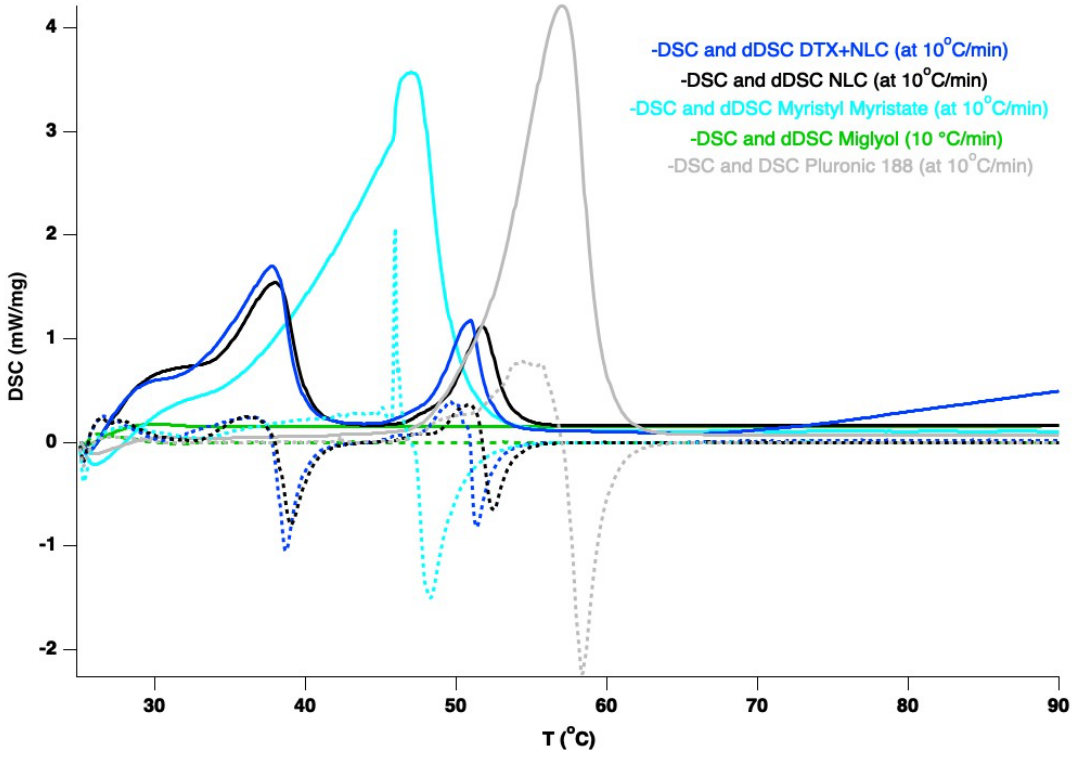

(b)

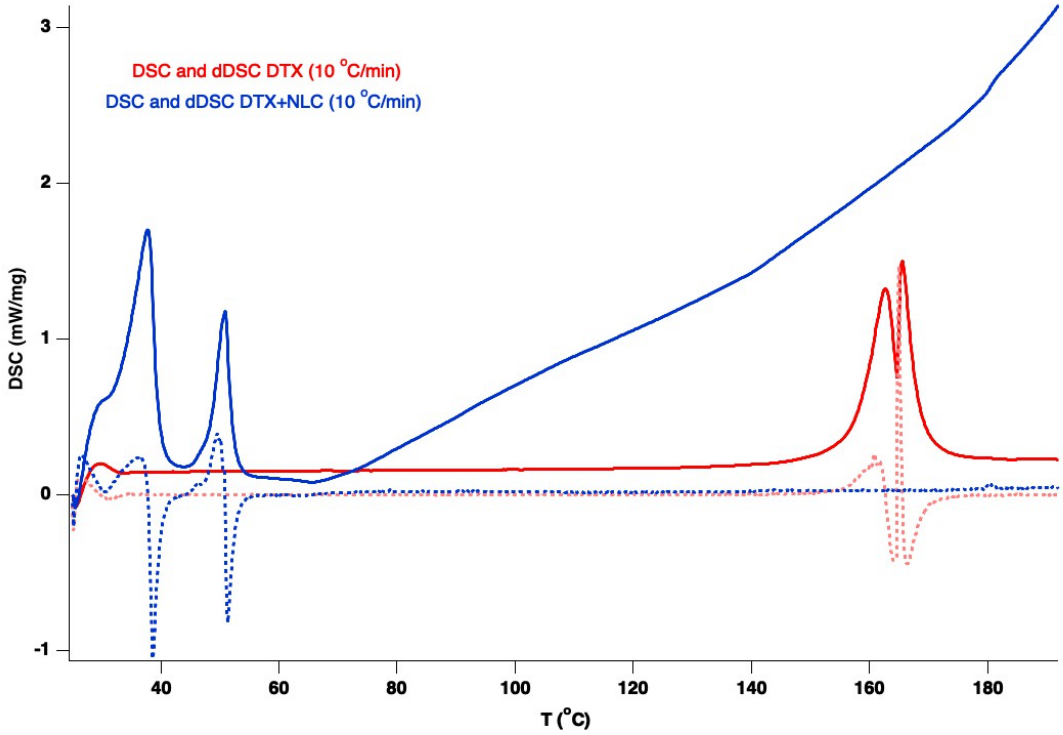

Figure 3.7: DSC curve obtained by heating DTX (red lines), DTX+NLC complex (dark blue lines), NLC (black lines), Myristyl Myristate (cyan lines), Miglyol (green lines) and Pluronic 188 (grey lines) from ambient temperature until 192℃ at a heating rate of 10 $\frac{℃}{min}$. Figures are highlighted in temperature intervals in order to capture the different phace transitions that happen.

Table 3: Melting points for each of the compounds of the DTX+NLC complex

Sample name	Melting points (℃)
DTX	162.7 and 165.6
Myristil Myristate	47.0
Miglyol[41]	-5.3
Pluronic	57.0
DTX+NLC	37.8 and 50.9
NLC	38.0 and 51.7

3.2.1.3 Applying the Kissinger model to DTX+NLC

(a)

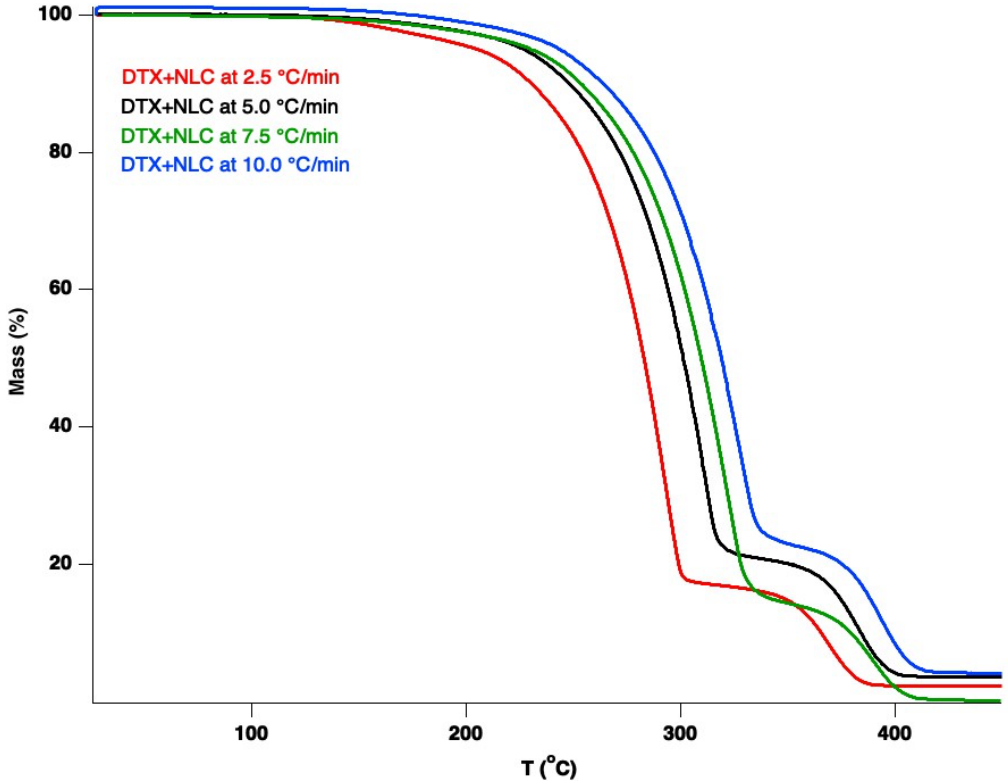

(b)

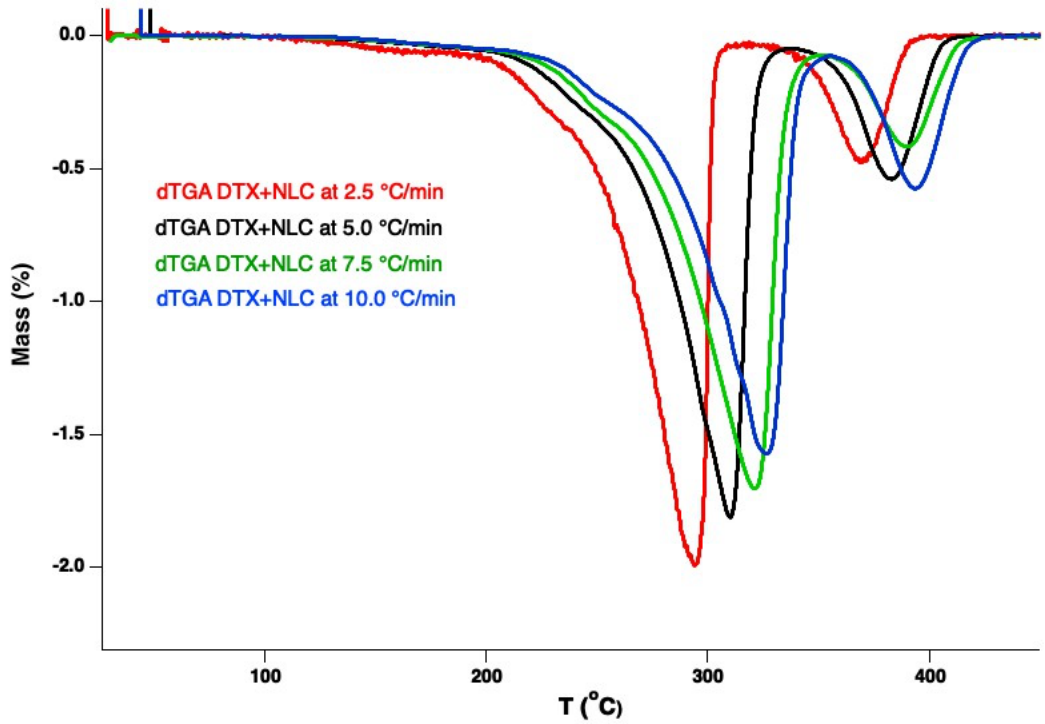

Figure 3.8: (a): Mass loss curves (TGA) of DTX+NLC using four different rates from ambient temperature until 450 ℃. Note the ordering of the curves going from the lowest rate losing the most mass per ℃ to the highest rate losing the least mass per ℃. (b): Differential of the mass loss curves(dTGA) for DTX+NLC . The differential sets clearer the rate of mass loss per ℃.

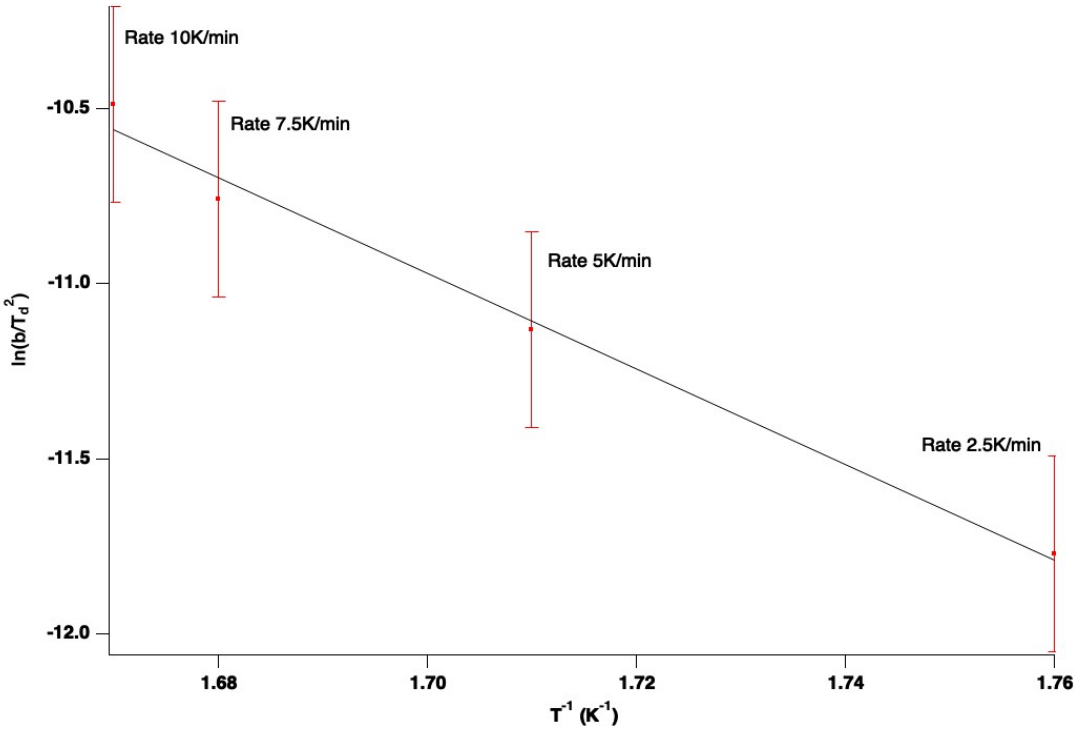

Figure 3.9. The Kissinger plot with a fitted line for the first minima corresponding to the decomposition of DTX+NLC for four different rates(2.5K/min, 5.0K/min, 7.5K/min and 10.0K/min) . The straight line shows a fit to the four data points, and the slope of this line is used to calculate the activation energy, as described in Section 2.3.2.

The results of the Kissinger model for the DTX+NLC complex show an increase of 5.3% in the activation energy for the first step of the decomposition processes. The higher value of the activation energy indicates higher stability of the encapsulated DTX molecules because more energy is needed in order to observe decomposition.

Table 4: Activation energy of the decomposition reaction obtained using the Kissinger model for the DTX+NLC complex. Further information we collect from this table is the starting point of decomposition as well as the percentage of the mass loss after the decomposition reaction.

$\mathbf{T_{rate}}$ $(\frac{℃}{min})$	T_d (℃) (Inset of decomposition)	$T_d^{-1} \times 10^{-3}(K)$	% mass loss	Activation Energy (kJ/mol)
2.5	295.4	1.76	82.72	-
5.0	311.4	1.71	78.59	-
7.5	321.9	1.68	85.42	-
10.0	325.7	1.67	77.83	-
-	-	-	-	113.35

3.2.2 Fourier Transformed Infrared Spectroscopy (FTIR) analysis connecting the results

The FTIR spectra analysis revealed some very interesting results. By looking at the infrared spectroscopy of the whole complex (drug + nanostructured lipid carriers, blue line) as well as the spectra of the DTX (red line) alone and the spectra of each compound of the NLC (Myristyl Myristate in cyan, Miglyol in green and Pluronic in grey color, respectively) as a function of temperature shown in Figure 3.8 , we are able to conclude that DTX is intercalated at least until 200 °C approximately. This is possible because FTIR spectroscopy gave us the ability to observe step by step in steps of 3.5 °C (approximately) the evolution of the decomposition of chemical components of each sample.

- **DTX**: We observed that for DTX a strong vibration in a wavelength range between (2250-2400 cm^{-1}) at 210 °C. This indicates decomposition of O=C=O (or N=C=O) of the sample while the complex is totally stable in this particular wavelength of that temperature interval. Moreover, a vibration starting below 60 °C which continuously appeared until around 81 °C in the spectral range corresponding to 1200- 1300 cm^{-1} can be attributed to the presence and releasing of ethanol (C_2H_5OH) of the sample. We know that the gas point of ethanol is on 78.38 °C and that alcohols have characteristic IR absorptions associated with both the O-H and the C-O stretching vibrations. The O–H stretch of alcohols appears in the region 3500-3200 cm^{-1} and is a very intense, broad band. The C–O stretch shows up in the region 1260-1050 $cm^{-1.}$ The spectrum of ethanol is also shown in Figure 3.10 [36].
- **DTX+NLC complex:** The first substance we observe to be released from the DTX+NLC complex is above 200 °C and it is associated to the myristil myristate decomposition that happens giving a huge peak in between 2800 and 3000 cm^{-1} and is associated to N-H (not sure) amine.

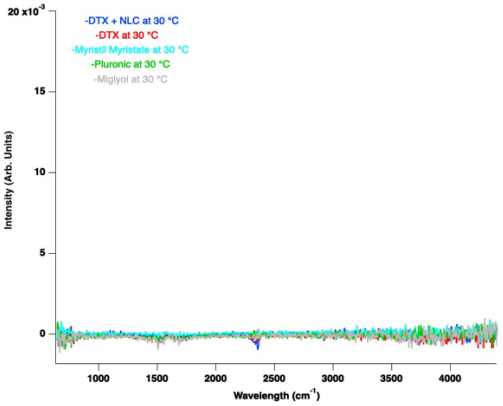
20 x10^-3
-DTX + NLC at 30 °C
-DTX at 30 °C
-Myristil Myristate at 30 °C
-Pluronic at 30 °C
-Miglyol at 30 °C
Intensity (Arb. Units)
Wavelength (cm^-1)

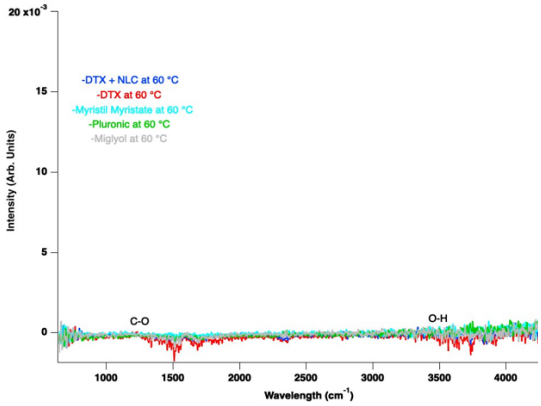
20 x10^-3
-DTX + NLC at 60 °C
-DTX at 60 °C
-Myristil Myristate at 60 °C
-Pluronic at 60 °C
-Miglyol at 60 °C
C-O
O-H
Intensity (Arb. Units)
Wavelength (cm^-1)

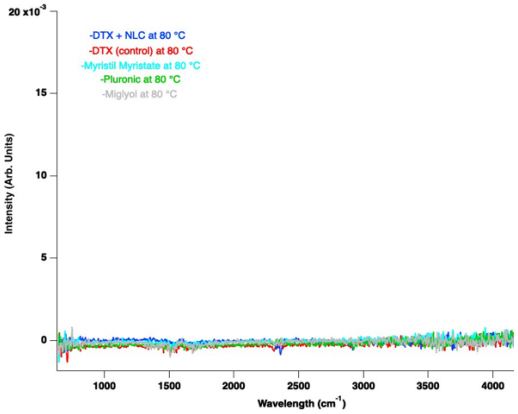
20 x10^-3
-DTX + NLC at 80 °C
-DTX (control) at 80 °C
-Myristil Myristate at 80 °C
-Pluronic at 80 °C
-Miglyol at 80 °C
Intensity (Arb. Units)
Wavelength (cm^-1)

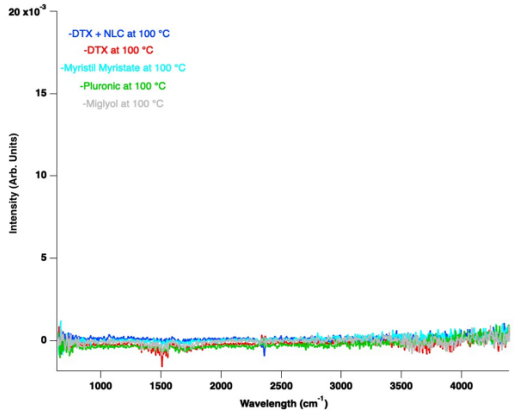
20 x10^-3
-DTX + NLC at 100 °C
-DTX at 100 °C
-Myristil Myristate at 100 °C
-Pluronic at 100 °C
-Miglyol at 100 °C
Intensity (Arb. Units)
Wavelength (cm^-1)

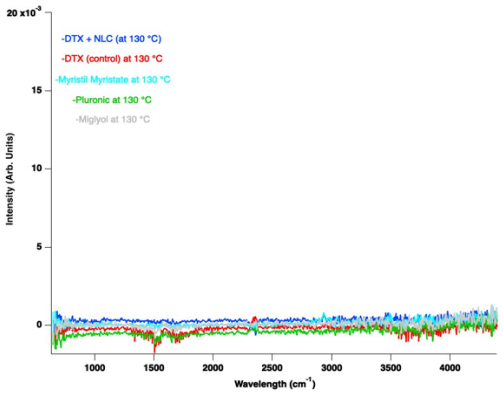
20 x10^-3
-DTX + NLC (at 130 °C)
-DTX (control) at 130 °C
-Myristil Myristate at 130 °C
-Pluronic at 130 °C
-Miglyol at 130 °C
Intensity (Arb. Units)
Wavelength (cm^-1)

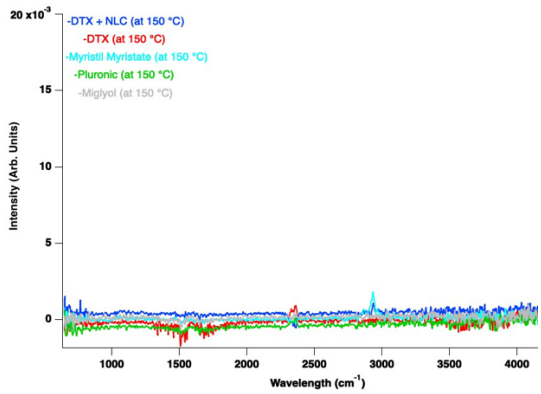
20 x10^-3
-DTX + NLC (at 150 °C)
-DTX (at 150 °C)
-Myristil Myristate (at 150 °C)
-Pluronic (at 150 °C)
-Miglyol (at 150 °C)
Intensity (Arb. Units)
Wavelength (cm^-1)

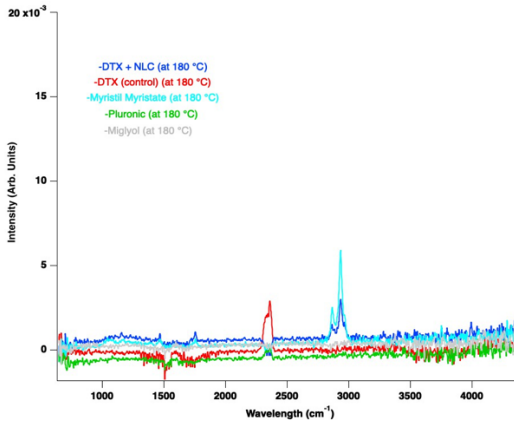
20 x10^-3
-DTX + NLC (at 180 °C)
-DTX (control) (at 180 °C)
-Myristil Myristate (at 180 °C)
-Pluronic (at 180 °C)
-Miglyol (at 180 °C)
Intensity (Arb. Units)
Wavelength (cm^-1)

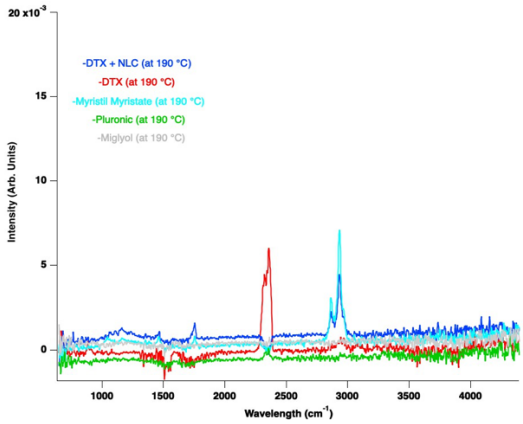
20 x10^-3
-DTX + NLC (at 190 °C)
-DTX (at 190 °C)
-Myristil Myristate (at 190 °C)
-Pluronic (at 190 °C)
-Miglyol (at 190 °C)
Intensity (Arb. Units)
Wavelength (cm^-1)

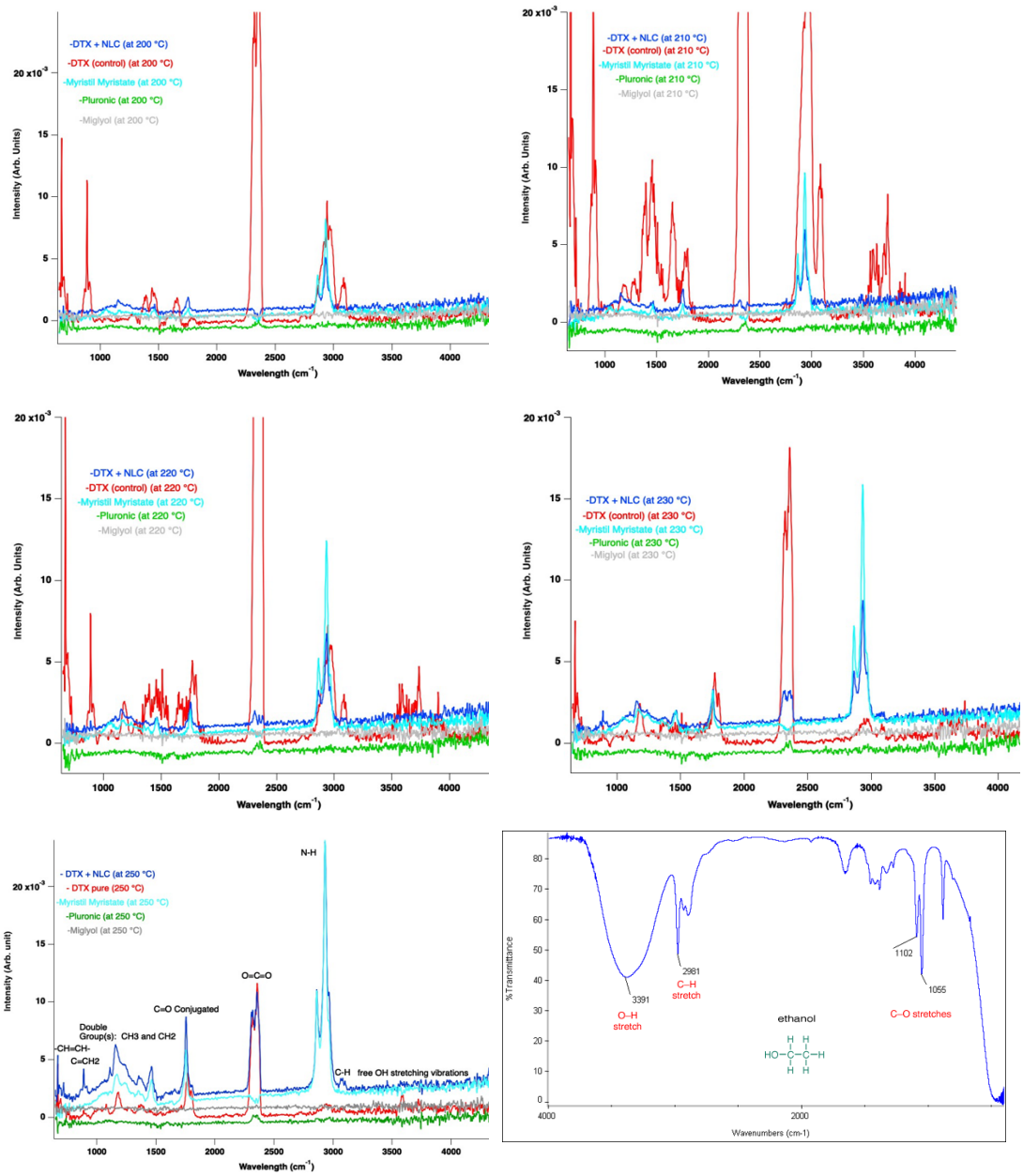

Figure 3.10: FTIR absorbance spectra of the DTX+NLC (dark blue) complex and each one separately of its components (DTX (red lines), Myristil Myristate (cyan lines), Miglyol (green lines) and Pluronic 188 (grey lines). At the bottom of the right side of the picture, the IR spectrum of ethanol is shown [37]. Data collected during the heating process in the apparatus up to 250 ºC at a heating rate of 10 ºC/min.

CHAPTER 4

Conclusion and outlook

With this project we focused on making a structural identification via scattering technique of an unknown polymorph of the anti-cancer drug DTX, complemented with a combination of thermal analysis and spectroscopy techniques. Further, we evaluated its encapsulation into a nanostructured lipid carrier composed of the Myristyl Myristate and Miglyol lipids (solid and liquid, respectively) and the Pluronic 188 surfactant.

The identification and thermal characterization of a polymorph drug is a crucial work in pharmaceutical research, because, under the biophysical approach we can point out differences in solubility, stability and other physicochemical properties among polymorphs.

The structural identification, via XRPD technique, showed the presence of two discrete structural forms in the material, consisting of an ethanol solvated and an anhydrous form. The FTIR spectroscopy provided additional information that the drug was solvated in ethanol, as the TG analysis showed a mass loss of 1.5%, vastly due to ethanol evaporation. Moreover, the DSC curve confirmed the presence of two discrete forms by a double consecutive peak at 162.7℃ and 165.6℃.

The results of our TG and FTIR spectrum analysis showed that the encapsulation was successful. By looking at the TG graph and the FTIR spectrum of the DTX as well as the FTIR spectrum of each one of the subcomponents, particularly, we observe releasing of some specific molecular units in temperatures below the 200 ℃. On the contrary, the spectra start showing peaks only after 200 ℃ , indicating that nothing was released/decomposed below that temperature.

Additionally, in order to evaluate the stability of the drug, we applied the Kissinger model, which provided the activation energy of the decomposition processes. Our results were very close to the reported results of activation energy of decomposition for drug- like molecules. We applied the model, also, in the DTX+NLC complex, when the drug was intercalated, and we got an increment around 5.3% in the activation energy for the first step of the decomposition of the complex. This fact clarified that the drug molecules appeared higher stability after the encapsulation, so, the drug was successfully encapsulated into the NLC.

Moreover, from our DSC data we get an absence of sharp phase transitions from around 55℃- 60℃ until 192℃ for the DTX+NLC complex, while we see, as we already mentioned, two very close to each other melting peaks for the drug alone. We only observe a gradually increased exothermic phase transition for the complex. The loss of these sharp peaks underlines amorphization or complexation of the pure drug molecules.

Appendix

Mitosis: is the process of cell division, where a single cell (mother cell) is divided into two identical cells (daughter cells). Mitosis is a very important part of the cell cycle because it cares for the growth of the cells and for the replacing of depleted cells, leading to a correction pattern for the cells. Irregularities during the mitotic phase can result in DNA imperfections, leading to genetic disorders.

Apoptosis: in the apoptosis process, the cells that are not needed any more (unhealthy cells) separated from the healthy ones, they are collected in "packages", and they self-degraded. It is a form of programmed cell death, or "cellular suicide". It is different from necrosis, in which cells die due to injury. Apoptosis maintains balance in the body and eliminates, to a certain extent, cancerous and other kinds of unhealthy cells. [https://www.khanacademy.org/science/biology/developmental-biology/apoptosis-in-development/a/apoptosis]

Lipids: The primary component of nanostructure lipid carriers that govern drug loading capacity, prolong action and stability of the formulations is lipid. Solid lipids like fatty acids have been used for formulating NLC. Physiologically acceptable, biodegradable and non-toxic, lipids are preferred for preparation of lipid nanoparticles.

The type and structure of lipid affects various characteristics of nanocarriers. Solubility or partition coefficient of bioactives in the lipid has been suggested as the best fitting criteria for choosing a suitable lipid. Solubility of the drug molecules in lipid affects drug loading and encapsulation efficiency. Degree of crystallization of various lipids employed also affect drug entrapment and loading, size and charge, and efficacy. Shape of lipid crystals, lipid hydrophilicity, variation in composition are additional parameters of the lipids, that may influence quality of NLC.

Ultrasonication: this is one of the methods to produce NLCs is the ultrasonication method. These dispersing techniques employ devices to prepare nanocarriers. Solid and liquid lipid is melted and dispersed in an aqueous surfactant solution under high shear homogenization or ultrasonication resulting in formation of nanodispersion. Intense shear forces necessary for the nano-emulsification are generated by ultrasonic cavitation which produces violently and asymmetrically imploding vacuum bubbles and break up particles down to the nanometer scale.

Probe-type ultrasonication produces desired effects like homogenization, dispersion, and deagglomeration. The type and concentration of lipid and surfactant, their ratio, time of sonication or agitation, speed are some of the parameters to be optimized to obtain a reproducible method resulting small size nanocarriers. Low dispersion quality is a disadvantage of high shear homogenization and ultrasonication. Dispersion quality of the lipid nanoparticles produced by these techniques is often affected by the presence of microparticles leading to physical instability upon storage. Metal contaminations from the equipment is the other important problem associated with ultrasonication.

Electrophoresis: is the motion of dispersed particles relative to a fluid under the influence of a spatially uniform external electric field. The technique requires the interface between the particles and the surrounding fluid to be charged. It is a laboratory technique used for separating molecules by size, charge, or binding affinity.[18]

Surfactants: Surfactants largely influence the toxicity, physical stability, and crystallinity of NLCs. They, also, have an impact on extent of drug dissolution and drug permeability. Surfactants are chosen based on of route of administration, hydrophilic-

lipophilic balance (HLB) value, effect on particle size and lipid modification. Surface active agents (emulsifiers) are adsorbed on the interface where they reduce the tension between lipid and aqueous phases because of their amphipathic nature. During the formulation of NLC, crystallization of colloid particles goes along with solidification, but the surface area of particle increases remarkably during crystallization so that the whole system becomes unstable. Hence, surfactant is a requisite to improve interface quality of nanoparticles to get stability. Modifying the surfactant system compositions may govern the miscibility of chemical components in NLCs, and hence the stability.

Ester: An ester is a chemical compound derived from an acid in which at least one –OH hydroxyl group is replaced by an O– alkyl group.

Bibliography:

[1] https://www.nhs.uk/conditions/breast-cancer/

[2] https://www.ema.europa.eu/en/medicines/human/EPAR/docetaxel-teva

[3] Liana Vella- Zarb et. al., *The Devil is in the Detail: A rare H- Bonding Motif in New Forms of Docetaxel*, dx.doi.org/10.1021/cg400814a | Cryst. Growth Des., 13, 4402−4410, 2013

[4] Sabina Tabaczar et al., *Molecular mechanisms of antitumor activity of taxanes. I. Interaction of docetaxel with microtubules*, 64:568-81, Nov. 19, 2010

[5] Jin-Seok Choi et al., *Development of docetaxel nanocrystals surface modified with transferrin for tumor targeting*, 11:17-26, 2017

[6] Ma and Mumper, *Lipids- Advances in Research and Application*, 2013

[7] Urmila Sri Syamala, US. *Calculation of MTDSC signals, factors effecting the signals and applications in drug development*. MOJ Bioequiv Availab. 2018;5(3):144-152. DOI: 10.15406/mojbb.2018.05.00095

[8] https://www.ccdc.cam.ac.uk/solutions/csd-core/components/mercury/

[9] https://en.wikipedia.org/wiki/Taxus_baccata

[10] Shinji Kuroda et. al., *Gene Therapy of Cancer (Third Edition),* Pages 171-183, 2014

[11] https://en.wikipedia.org/wiki/Docetaxel

[12] Iti Chauhan, Mohd Yasir, Madhu Verma, Alok Pratap Signh, *Nanostructured Lipid Carriers: A groundbreaking Approach for Transdermal Drug Delivery*, Adv. Pharm. Bull., 10(2), 150-165, 2020

[13] Kaur S, Nautyal U, Singh R, Singh S, Devi A., *Nanostructure lipid carrier (NLC): the new generation of lipid nanoparticles*. Asian Pac J Health Sci. 2015;2(2):76–93. doi: 10.21276/apjhs.2015.2.2.14.

[14] https://www.larodan.com/product/myristyl-myristate/

[15] https://en.wikipedia.org/wiki/Triglyceride

[16] http://www.astonchem.com/pro_result/544513/

[17] Bing Guan et al., *Characterization of poloxamers by reversed-phase liquid chromatography*, 2015

[18]https://www.drugfuture.com/Pharmacopoeia/USP32/pub/data/v32270/usp32nf27s0_m66210.html

[19] Hery Mitsutake et al., *Thermal analysis and spectroscopic techniques to investigate docetaxel polymorphism*, 2021

[20] Norio Iwashita, *Materials Science and Engineering of Carbon Characterization*, 2016].

[21]https://serc.carleton.edu/research_education/geochemsheets/techniques/XRD.html

[22]https://chem.libretexts.org/Bookshelves/Analytical_Chemistry/Supplemental_Modules_(Analytical_Chemistry)/Instrumental_Analysis/Diffraction_Scattering_Techniques/Powder_X-ray_Diffraction

[23]https://www.bruker.com/en/products-and-solutions/diffractometers-and-scattering-systems/x-ray-diffractometers/d8-discover-family/d8-discover-plus.html?campaign=Discover-NA-EU-(XRD)&source=google&medium=cpc&keyword=x%20ray%20angle&device=c&gclid=Cj0KCQjws-OEBhCkARIsAPhOkIaC2qQr442B8Bqms3xiIqNi1YBuuGcrzXurJckLY2M_ccE30D-VnQoaAo_6EALw_wcB

[24] Smith, B. C., *Fundamentals of Fourier Transform Infrared Spectroscopy*, 2nd edn. Boca Raton, FL: CRC Press, 2011

[25] Margaris, A. V., Fourier Transform Infrared Spectroscopy (FTIR): applications in archaeology. In Smith, C. (ed.), *Encyclopedia of Global Archaeology*. New York: Springer, pp. 2890–2893, 2014

[26] Francesco Berna, Fourier Transformed Infrared Spectroscopy (FTIR), First Online: 12 August 2016

[27] TG- FTIR- An Integrated Approach to Thermal Analysis, Sponsored by Bruker optics, Feb. 12 2012

[28] https://h-and-m-analytical.com/wp/decomposition-analysis-calcium-oxalate-using-tga/

[29] Homer E. Kissinger, Variation of Peak Temperature With Heating Rate in Differential Thermal Analysis, Journal of Research of the National Bureau of Standards, Vol. 57, No. 4, Oct. 1956

[30] Pooria Gill et al., Differential Scanning Calorimetry Techniques: Applications in Biology and Nanoscience, J Biomol Tech., 21(4): 167-193, 2010

[31] Haines PJ, Reading M, Wilburn FW. Differential thermal analysis and differential scanning calorimetry. In Brown ME. (ed): *Handbook of Thermal Analysis and Calorimetry*, vol 1 The Netherlands: Elsevier Science BV, 279–361, 1998

[32] Danley RL. New heat flux DSC measurement technique. *Thermochim Acta*, 395:201–208, 2002

[33] https://www.netzsch-thermal-analysis.com/en/products-solutions/differential-scanning-calorimetry/dsc-214-polyma/

[34] L. Zaske, M.-A. Perrin et F. Leveiller, *Docetaxel: Solid state characterization by X-ray powder diffraction and thermogravimetry*, J. Phys. IV France 11, 2001

[35] https://products.sanofi.ca/en/taxotere.pdf

[36] https://orgchemboulder.com/Spectroscopy/irtutor/alcoholsir.shtml

[37] https://orgchemboulder.com/Spectroscopy/irtutor/alcoholsir.shtml

[38] Lakshimi Kumar Tatini, K. V. S. R. Krishna Reddy, and N. Someswara Rao, *Vapor- Induced Phase Transformations in Docetaxel*, AAPS PharmSciTech, Vol. 13, No. 2, June 2012

[39] Philip A. MacFaul, Linette Ruston and J. Matthew Wood, *Activation energies for the decomposition of pharmaceuticals and their application to predicting hydrolytic stability in drug discovery*, Med. Chem. Commun., 2011, 2, 140-142

[40] Tatini *et al.*, AAPS PharmSciTech 13, 548-555 (2012)

[41] C. Puglia et al., *International Journal of Pharmaceutics*, 357, (2008), 295–304

[42] M.L. Martins et al*., International Journal of Pharmaceutics*, 524, (2017), 397–406